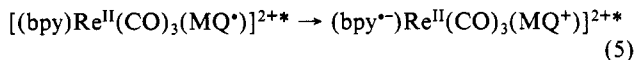


loss associated with the transition between states is offset by a gain in energy in the intramolecular vibrations (eq 3).

On the other hand, if $(\Delta G_{es,2} + \lambda_{0,2}) > (\Delta G_{es,1} + \lambda_{0,1})$ (Figure 4B) and nuclear tunneling effects in the librational modes are unimportant, intramolecular electron transfer can not occur in a frozen environment. The situation is the same as in Figure 3A. Even direct $\text{Re(I)} \rightarrow \text{MQ}^+$ excitation (process a in Figure 4B) must either lead to the ground state by emission or to the $\text{Re(II)}-\text{bpy}^*$ -based MLCT state by reverse electron transfer:



The inversion in the sense of the electron transfer in the frozen environment is induced energetically by the greater solvent reorganizational energy for the lower excited state, $\lambda_{0,2} > \lambda_{0,1} - (\Delta G_{es,2} - \Delta G_{es,1})$.

In a macroscopic sample, a distribution of solvent dipole environments exists around the assembly of ground states. For some of the high-energy distributions, vertical $\text{Re(I)} \rightarrow \text{bpy}$ excitation may lead to or beyond the intersection point of the $\text{Re(II)}(\text{bpy}^*)$ and $\text{Re(II)}(\text{MQ}^*)$ potential energy curves shown in Figure 4B. For such cases, unusual excitation energy effects may exist for chromophores surrounded by solvent dipole distributions of sufficiently high energy. Such phenomena are difficult to observe by emission measurements in $[(\text{bpy})\text{Re}(\text{CO})_3(\text{MQ}^*)]^{2+}$. For this complex, the energy difference between the two excited states is relatively small and the $\text{Re}^{\text{II}}-\text{bpy}^*$ -based emission is far more intense than $\text{Re}^{\text{II}}-\text{MQ}^*$ -based emission. However, excitation energy effects are observed for $[(4,4'-(\text{NH}_2)_2-\text{bpy})\text{Re}(\text{CO})_3(\text{MQ}^*)]^{2+}$. For the amino derivative, a residual high-energy $\text{Re}^{\text{II}}-[4,4'-(\text{NH}_2)_2-\text{bpy}^*]$ -based emission can be observed, but only at relatively high excitation energies (Figure 2C). The excitation leading to $\text{Re}^{\text{II}}-[4,4'-(\text{NH}_2)_2-\text{bpy}^*]$ emission is shown as process c in Figure 4A. At lower excitation energies, the high-energy emission disappears and only the broad, lower energy emission from the $\text{Re}^{\text{II}}-\text{MQ}^*$ -based excited state is observed.

For the $\text{Re}(\text{MQ}^*)$ -based complexes an additional complication to intramolecular electron transfer exists arising from a "flattening" of the relative orientations of the two rings of the MQ^+ ligand when it accepts an electron.¹⁴⁻¹⁶ However, the analysis presented here does provide a general explanation for the role of free energy change in environments where dipole motions are restricted. For a directed, intramolecular electron transfer such as reaction 1, the change in electronic distribution between states will, in general, lead to a difference between $\lambda_{0,1}$ and $\lambda_{0,2}$. This difference creates a solvent dipole barrier to intramolecular electron transfer. It follows from eq 4 that if light-induced electron transfer is to occur in a frozen environment, the difference in solvent reorganizational energy, $\Delta\lambda_0 = \lambda_{0,2} - \lambda_{0,1}$, must be compensated for by a favorable free energy change, $\Delta(\Delta G) = \Delta G_{es,2} - \Delta G_{es,1}$, as

$$\Delta G_{es,1} - \Delta G_{es,2} > \lambda_{0,2} - \lambda_{0,1}$$

or

$$-\Delta(\Delta G) > \Delta\lambda_0$$

Presumably, this condition is met in the reaction center.¹⁷ There the free energy change is favorable and the surrounding dipole reorganizational energies are small. The low polarity of the surrounding environment minimizes the magnitude of $\Delta\lambda_0$.

Acknowledgment. Acknowledgement is made to the National Science Foundation for financial support under Grant CHE-8503092.

(15) (a) Swiatkowski, G.; Menzel, R.; Rapp, W. *J. Lumin.* **1987**, *37*, 183. (b) Yamaguchi, S.; Yoshimizu, N.; Maeda, S. *J. Phys. Chem.* **1978**, *82*, 1078.

(16) (a) Knyazhanski, M. I.; Feigelman, V. M.; Tymyanski, Y. R. *J. Lumin.* **1987**, *37*, 215. (b) Barker, D. J.; Cooney, R. P.; Summers, L. A. *J. Raman Spectrosc.* **1987**, *18*, 443. (c) Hester, R. E.; Suzuki, S. *J. Phys. Chem.* **1982**, *86*, 4626.

(17) (a) Parson, W. W. In *Photosynthesis*; Ames, J., Ed.; Elsevier: Amsterdam, 1987; Chapter 3, p 43. Won, Y.; Friesner, R. A. *Proc. Natl. Acad. Sci. U.S.A.* **1987**, *84*, 5511. (c) Creighton, S.; Hwang, J.-K.; Warshel, A.; Parson, W. W.; Norris, J. *Biochemistry* **1988**, *27*, 774. (d) Gunner, M. R.; Robertson, D. E.; Dutton, P. L. *J. Phys. Chem.* **1986**, *90*, 3787.

FEATURE ARTICLE

Classical and Modern Methods in Reaction Rate Theory

Bruce J. Berne,* Michal Borkovec,[†] and John E. Straub[‡]

Department of Chemistry, Columbia University, New York, New York 10027 (Received: February 9, 1988)

The calculation of chemical reaction rate constants is of importance to much of chemistry and biology. Here we present our current understanding of the physical principles determining reaction rate constants in gases and liquids. We outline useful theoretical methods and numerical techniques for single- and many-dimensional systems, both isolated and in solvent, for weak and strong collision models and discuss connections between different theories from a unified point of view. In addition, we try to indicate the most important areas for future work in theory and experiment.

1. Introduction

The influence of solvents on rate constants of chemical reactions has been studied for over a century and has recently received renewed attention.¹⁻⁵ A clear physical picture of how solvents

influence the rate of chemical reactions is beginning to emerge. This feature article presents our personal view of classical, as well

* Present address: Institut für Physikalische Chemie, Universität Basel, Klingelbergstr. 80, 4056 Basel, Switzerland.

[†] Present address: Department of Chemistry, Harvard University, Cambridge, MA 02138.

(1) Kramers, H. A. *Physica* **1940**, *7*, 284.
(2) Truhlar, D. G.; Hase, W. L.; Hynes, J. T. *J. Phys. Chem.* **1983**, *87*, 2664.

(3) Hynes, J. T. *Annu. Rev. Phys. Chem.* **1985**, *36*, 573.

(4) Hynes, J. T. In *Theory of Chemical Reaction Dynamics*; Baer, M., Ed.; CRC Press: Boca Raton, FL, 1985; p 171.

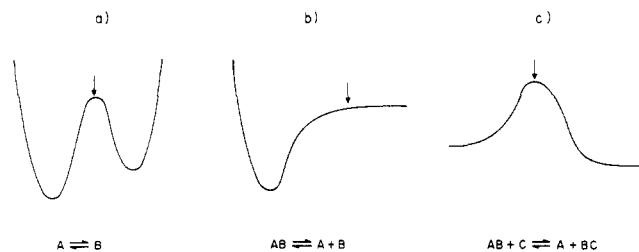


Figure 1. Schematic representation of the reaction coordinate potential for (a) isomerization, (b) recombination, and (c) atom-transfer reactions. The arrow denotes the dividing surface.

as modern, theories of chemical reaction rate constants.

It is useful to classify common chemical reactions into three types: isomerization reactions, dissociation–recombination reactions, and atom-transfer reactions (see Figure 1). Isomerization reactions are unimolecular whereas atom-transfer reactions are bimolecular. In dissociation–recombination reactions, the dissociation step is unimolecular but the recombination step is bimolecular. The potential energy surfaces, as a function of the reaction coordinate, have a characteristic structure for each reaction type. Isomerization reactions correspond to transitions between metastable wells in a double or multiple minima potential (Figure 1a). Dissociation–recombination reactions involve a transition between a metastable well and isolated species in a single minimum potential (Figure 1b). In atom-transfer reactions, the potential energy surface has a barrier as a function of the reaction coordinate but no metastable wells (Figure 1c).

We can distinguish reactants from products by asking whether they lie to the left or right of a dividing surface (arrows in Figure 1) known as the transition state.⁶ The precise position of this surface is unimportant for the exact calculation of the rate constant provided the barrier separating the metastable species is high enough. Reactants of unimolecular reactions are bound, i.e., surrounded by potential walls, whereas reactants undergoing bimolecular reaction are not. The ratio of the rate constant for the forward reaction to the rate constant for the backward reaction is related to the equilibrium constant by detailed balance.

To make this more explicit, let us mention a few prototypical examples. Trans–gauche isomerization of butane represents an isomerization reaction.^{7–9} Here the reaction coordinate is the dihedral angle which moves on a periodic tristable potential curve and the dividing surface is located at the trans–gauche barrier. In the iodine dissociation–recombination reaction the reaction coordinate is the bond length^{10,11} which moves on a Morse-like potential curve; the dividing surface is located at a distance of a few equilibrium bond lengths. Finally, a typical atom-transfer reaction is a hydrogen exchange reaction.¹² In the simplest case, the reaction coordinate is the difference in the bond lengths moving on a Porter–Karplus-like surface and the dividing surface is characterized by equal bond lengths.

Important classical theories for calculating rate constants can be divided into three groups: transition-state theory,⁶ unimolecular rate theory in gases,¹³ and the theory of diffusion-controlled reactions.^{4,14} Transition-state theory assumes that there is equilibrium between the reactant A and an activated transition state A* which decomposes with a characteristic vibrational frequency

(5) Hänggi, P. *J. Stat. Phys.* **1985**, *42*, 105. Addendum and Erratum, *Ibid.* **1986**, *44*, 1003.

(6) Pechukas, P. In *Dynamics of Molecular Collisions, Part B*; Miller, W. H., Ed.; Plenum: New York, 1976.

(7) Berne, B. J.; DeLeon, N.; Rosenberg, R. O. *J. Phys. Chem.* **1982**, *86*, 2166.

(8) Montgomery, J. A., Jr.; Chandler, D.; Berne, B. J. *J. Chem. Phys.* **1979**, *70*, 4056.

(9) Montgomery, J. A., Jr.; Holmgren, S. L.; Chandler, D. *J. Chem. Phys.* **1980**, *73*, 3866.

(10) Hynes, J. T.; Kapral, R.; Torrie, G. M. *J. Chem. Phys.* **1980**, *72*, 177.

(11) Borkovec, M.; Berne, B. J. *J. Phys. Chem.* **1985**, *89*, 3994.

(12) Garrett, B. C.; Truhlar, D. J. *J. Am. Chem. Soc.* **1980**, *102*, 2559.

(13) Forst, W. *Theory of Unimolecular Reactions*; Academic: New York, 1973.

(14) Calef, D. F.; Deutch, J. M. *Annu. Rev. Phys. Chem.* **1983**, *34*, 493.

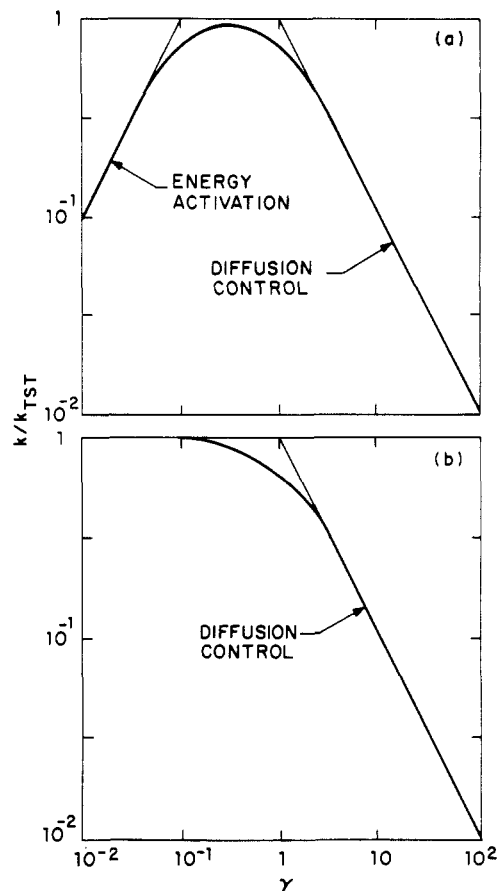
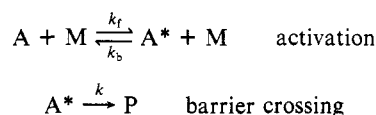


Figure 2. Log-log plot of the transition-state theory normalized rate constant as a function of the static friction constant γ typical of (a) an isomerization or dissociation–recombination reaction and (b) an atom-transfer reaction.

to products. The resulting rate constant, which is an upper bound on the true rate constant, depends on the properties of the reactant and on the solvent density only through the potential of mean force.

Transition-state theory (TST) does not explain the behavior of unimolecular reactions at low pressures; Lindemann proposed a mechanism for the activation of the reactant¹³ which describes



a unimolecular reaction proceeding in two steps. First, a reactant A is activated by a collision with a solvent molecule M; i.e., it acquires enough energy to cross the barrier. Second, the activated reactant A* crosses the barrier region to become product P.

Assuming that [A*] reaches a steady state, the rate constant for the formation of the product is

$$k(M) = k \frac{k_f[M]}{k + k_b[M]} \quad (1.1)$$

At very low pressures, or very small k_b such that $k \gg k_b[M]$, $k(M) = k_f[M]$ increases linearly with [M] or collision rate; collisions with solvent are infrequent and the activation step is rate limiting. At high pressures, such that $k \ll k_b[M]$, $k(M) = k k_f/k_b$ and the rate constant becomes independent of the collision rate. In this limit, the theory of unimolecular reactions reduces to TST. The theory of unimolecular reactions predicts that at low pressures the rate constant increases linearly with the solvent density and becomes independent of the density at high pressures.

However, it is often noted that as the density of the solvent, and the solvent viscosity, increases, the reaction rate constant decreases. In this case, the crossing of the barrier is strongly hindered by frequent collisions with the solvent and the rate

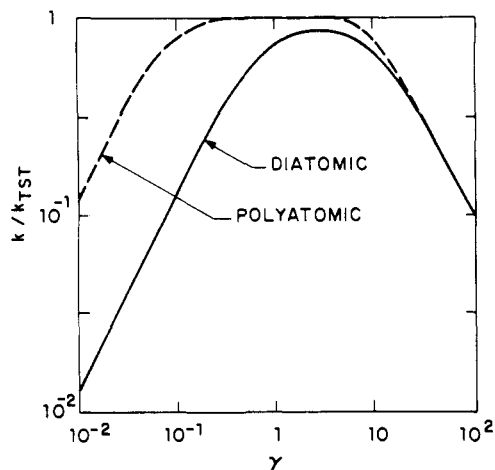


Figure 3. Log-log plot of the transition-state theory normalized rate constant as a function of the static friction constant γ for a diatomic (—) and a polyatomic (---) molecule.

constant is proportional to the diffusion coefficient which decreases with solvent density.

By continuously increasing the density of the solvent from a dilute gas to a dense liquid, the system will pass through the energy activation regime to the diffusion-controlled regime. Each process can act as the rate-limiting step and the rate constant displays a maximum (turnover). This was recognized by Kramers¹ in his seminal attempt to treat all these different models within the same theoretical framework and is a topic of active research interest today.

The rate constant of an isomerization or dissociation-recombination reaction, as a function of the friction constant, will therefore behave in the characteristic fashion shown in Figure 2a. In a low-density gas, the rate constant will increase in proportion to the friction or collision rate due to energy activation. In a dense solvent, it will be proportional to the diffusion coefficient, or inversely proportional to the friction, and therefore will decrease with increasing density. In between, it will go through a maximum which will lie below the value given by transition-state theory.

The physical reason that the recombination rate constant vanishes at zero pressure is that an incoming trajectory will always rebound from the repulsive potential wall and will therefore always be unreactive. For atom-transfer reactions, the situation is different. No repulsive wall is present in this case (see Figure 1) so that such a trajectory will always have a nonvanishing rate constant. Therefore, in an atom-transfer reaction the energy activation step is missing and the rate constant will be given by transition-state theory at low pressures. Again, in dense solvents diffusion control will cause the rate constant to decrease (see Figure 2b). *In summary, rate constants for atom-transfer reactions simply decrease as a function of density whereas isomerization reactions and dissociation-recombination reactions first increase and then decrease, showing a maximum (turnover) as a function of the solvent density.* The maximum is sharp for a diatomic reaction and very broad for a polyatomic reaction (Figure 3). Of course, nature is often complex and several effects modify this simple picture of chemical reactions. The most important are equilibrium solvent effects, non-RRKM effects, and non-Markovian effects.

First, equilibrium solvent effects modify the interaction potential and thereby the barrier height and frequency, which in turn affects the rate constant. At low pressures and high temperatures the pressure dependence of the transition-state rate constant is characterized by a constant reaction volume—the volume difference between the molecule in the transition state and in the reactant state.¹⁵ In dense or strongly interacting solvents, this effect arises from many-body interactions with the solvent.¹⁵ In some cases the bare potential can be replaced by the potential of

(15) Pratt, L. R.; Hsu, C. S.; Chandler, D. *J. Chem. Phys.* **1978**, *68*, 4202.

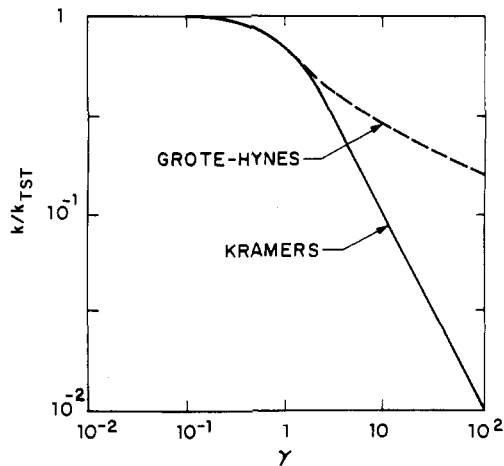


Figure 4. Log-log plot of the transition-state theory normalized rate constant as a function of the static friction γ for Markovian (—) and non-Markovian (---) friction where the correlation time increases with γ , which is typical for liquids.¹¹⁶

mean force, the quantity that specifies how the free energy changes as the reaction coordinate changes. Strong dependence of the TST reaction rate of polar solutes on the dielectric constant of the solvent is an example of this effect.¹⁶

Second, non-RRKM effects modify the initial rise of isomerization and dissociation-recombination reaction rates at low to intermediate densities. The strong enhancement of the low-pressure rate constant with increasing number of degrees of freedom of the molecule is based on the assumption of RRKM theory that the vibrational modes are very strongly coupled leading to fast energy equipartitioning and intramolecular vibrational relaxation (IVR).^{13,17} However, as the number of degrees of freedom of the molecule increases, the coupling between modes will decrease so that the assumption of fast IVR may be violated.^{18,19} Moreover, correlated recrossings of the transition state related to the topology of phase space can lead to profound deviations from statistical theories like RRKM theory.^{7,20-26}

Third, non-Markovian effects first discussed by Grote and Hynes²⁷ weaken or even suppress the transition to diffusion control in dense solvents for any reaction type.⁴ The physical origin of this effect lies in the observation that a realistic solvent takes a finite relaxation time to adjust to the motion of the solute. If the relaxation time is short, the solvent exerts a very rapidly fluctuating force on the reaction coordinate which thus experiences a large, Markovian friction.^{1,28} This leads to a reduction of the rate constant due to diffusion control (Figure 4). However, most realistic solvents do not relax quickly. When the relaxation time is very long, the solvent exerts such a slowly fluctuating force that the reaction coordinate moves in an approximately constant force field. It then experiences very little friction and will therefore be less affected by the solvent. In this limit, transition-state theory might be valid at much higher friction than the diffusion-controlled model would predict.

In this feature article we will address these topics in more detail. In section 2 we discuss transition-state theory, and section 3 outlines new numerical methods for the calculation of rate constants. In section 4 we discuss unimolecular rate theory, and in

(16) Hicks, J.; Vandersall, M.; Babarogic, Z.; Eissenthal, K. *Chem. Phys. Lett.* **1985**, *116*, 18.

(17) Troe, J. *Annu. Rev. Phys. Chem.* **1978**, *29*, 223.

(18) Rice, O. K. *Z. Phys. Chem. B* **1930**, *7*, 226.

(19) Hase, W. L. In *Dynamics of Molecular Collisions, Part B*; Miller, W. H., Ed.; Plenum: New York, 1976.

(20) DeLeon, N.; Berne, B. J. *J. Chem. Phys.* **1981**, *75*, 3495.

(21) DeLeon, N.; Berne, B. J. *J. Chem. Phys.* **1982**, *77*, 283.

(22) DeLeon, N.; Berne, B. J. *Chem. Phys. Lett.* **1982**, *93*, 162.

(23) DeLeon, N.; Berne, B. J. *Chem. Phys. Lett.* **1982**, *93*, 169.

(24) Davis, M. J. *J. Chem. Phys.* **1985**, *83*, 1016.

(25) Davis, M. J.; Gray, S. K. *J. Chem. Phys.* **1986**, *84*, 5389.

(26) Gray, S. K.; Rice, S. A. *J. Chem. Phys.* **1987**, *87*, 2020.

(27) Grote, R. F.; Hynes, J. T. *J. Chem. Phys.* **1982**, *77*, 3736.

(28) Smoluchowski, M. *Z. Phys. Chem.* **1918**, *92*, 129.

section 5 we consider diffusion-controlled reactions and Grote-Hynes theory. We discuss connection formulas, electronic surface crossing, and computer simulations in section 6 while section 7 reviews experiments.

Several important topics could not be considered. There are some reactions, for example, the gauche⁺ to gauche⁻ reaction in butane, which belong to none of the three types discussed above. In such cases, the ideas presented do not necessarily apply although their generalization should be possible. We also do not discuss reactions where several reaction channels might compete with each other. While attempts have been made to include nonequilibrium effects,²⁹⁻³¹ we focus on chemical reactions near thermal equilibrium. While we briefly consider electronic surface crossing, quantum effects,^{5,32,33} which modify the motion of the nuclei, are not discussed.

2. Transition-State Theory

Transition-state theory is the most frequently used analytic theory for calculating rate constants.^{2,6} The following two sections provide a brief review of *microcanonical* transition-state theory for isolated molecules, or RRKM theory, developed mainly by Rice, Ramsberger, Kassel, and Marcus,¹³ and *canonical* transition state theory for reactions in solvents developed mainly by Wigner³⁴ and Eyring.³⁵

2.1. Microcanonical Transition-State Theory. For a constant energy ensemble, the forward transition-state theory rate constant is given by RRKM theory:^{19,36}

$$k_{\text{RRKM}}^{\text{f}}(E) = \frac{\langle \dot{x}\delta(x)\theta(\dot{x}) \rangle_E}{\langle \theta(-x) \rangle_E} \quad (2.1)$$

where $\delta(x)$ is the Dirac delta function and $\theta(x)$ the Heaviside step function. The reaction coordinate x is chosen so that it is positive for products and negative for reactants; i.e., the transition-state surface is placed at $x = 0$. The microcanonical average denoted by $\langle \dots \rangle_E$ is an average over phase space restricted to the energy shell E . Averaging $k_{\text{RRKM}}^{\text{f}}(E)$ over the canonical energy distribution results in the canonical transition-state theory rate constant.³⁶

RRKM theory assumes that all states with total energy E will react with equal probability and that trajectories crossing the transition state do not rapidly recross it. A necessary, but not sufficient, condition is that motion on the potential energy surface be ergodic. DeLeon and Berne^{20,21} proposed a statistical theory for isomerization reactions in nonergodic systems where one may decompose the full phase space into regions of regular and irregular motion. The irregular region may be defined as that region accessible to a set of trajectories originating at the transition-state surface.²² The rate constant was then shown to be²⁰

$$k_{\text{BD}}(E) = (\Omega(E)/\Omega_{\text{irr}}(E))k_{\text{RRKM}}(E) \quad (2.2)$$

where $\Omega(E)$ and $\Omega_{\text{irr}}(E)$ are respectively the full density of states and the density of states for the irregular region of the energy hypersurface at energy E . It follows from the definition that $k_{\text{BD}} \geq k_{\text{RRKM}}$. In most cases, the phase space is not metrically decomposable into distinct regular and irregular regions and (2.2) is only approximate. In a series of papers DeLeon and Berne^{7,20-23} explored how the presence of vague tori³⁷ in phase space affects the validity of RRKM theory. They showed that strong chaos is a necessary but not sufficient condition for RRKM theory to be valid. Moreover, they found that correlated recrossings give dynamic corrections which result in $k(E)$ being lower than predicted by (2.2). Berne showed how in a strong collision theory these dynamic effects are reflected in the variation of the rate

constant with collision rate at low collision rates; that is how these dynamic effects modify the unimolecular rate theory.³⁸

Recently, more detailed statistical theories describing non-RRKM effects have been developed by using the idea of phase-space bottlenecks, or Cantori, which form partial barriers between irregular regions of phase space.^{39,40} Studies have been completed for intramolecular energy transfer in OCS,²⁴ fragmentation of HeI₂,²⁵ and the isomerization model of DeLeon and Berne.²⁶ The approach is similar to variational transition-state theory in that it attempts to locate the optimal transition state: a bottleneck in phase space which forms a barrier to rapid equipartitioning. It provides a concrete mechanism for the underlying phase-space dynamics and appears to be the most promising avenue for studying the role of chaos in isolated and collisional reaction systems.

2.2. Canonical Transition-State Theory. The forward transition-state rate constant is given by^{6,41}

$$k_{\text{TST}}^{\text{f}} = \frac{\langle \delta(x)\dot{x}\theta(\dot{x}) \rangle}{\langle \theta(-x) \rangle} \quad (2.3)$$

where $\langle \dots \rangle$ is an equilibrium average over the canonical distribution function $e^{-\beta H}$, where H is the system Hamiltonian and $\beta = 1/k_{\text{B}}T$. By integrating over the velocities this formula^{42,43} can be expressed as an average over configurational coordinates only:

$$k_{\text{TST}} = \frac{1}{(2\pi\beta)^{1/2}} \frac{\langle \delta(x)\mu(\mathbf{r}) \rangle}{\langle \theta(-x) \rangle} \quad (2.4)$$

where

$$\mu(\mathbf{r}) = \left(\sum_i \frac{1}{m_i} \left(\frac{\partial x}{\partial r_i} \right)^2 \right)^{1/2} \quad (2.5)$$

The square of μ is the inverse "mass" of the reaction coordinate.⁴⁴

Often $\mu(\mathbf{r})$ depends very weakly on the configurational coordinates \mathbf{r} so that, to an excellent approximation, it can be replaced by its value at the saddle point \mathbf{r} . This simplifies the problem enormously since now (2.4) can be rewritten in terms of the configurational distribution function $S(x)$ as

$$k_{\text{TST}} \simeq \frac{\mu(\mathbf{r}_s)}{(2\pi\beta)^{1/2}} S(0) \quad (2.6)$$

$S(x)$ may be defined in terms of the potential of mean force $W(x)$ ⁴⁵ as^{7,46}

$$S(x_0) = \langle \delta(x - x_0) \rangle = \frac{e^{-\beta W(x_0)}}{\int_0^\infty dx e^{-\beta W(x)}} \quad (2.7)$$

which is simply the probability distribution function of x in a thermal ensemble. Equation 2.6 is the expression for the forward rate constant. The backward rate constant is given by the same expression except the integration limits in (2.7) are $-\infty$ and 0.

For unimolecular reactions (2.4) is simply the transition-state theory rate constant in units of inverse time. However, for a

(38) Berne, B. J. *Chem. Phys. Lett.* **1984**, *107*, 131.

(39) MacKay, R. S.; Meiss, J. D.; Percival, I. C. *Physica D (Amsterdam)* **1984**, *13D*, 55.

(40) Bensimon, D.; Kadanoff, L. P. *Physica D (Amsterdam)* **1984**, *13D*, 82.

(41) Chandler, D. J. *Chem. Phys.* **1978**, *68*, 2959.

(42) Wilson, E. B.; Decius, J. C.; Cross, P. C. *Molecular Vibrations*; Dover: New York, 1980.

(43) Borkovec, M.; Berne, B. J., unpublished results.

(44) This quantity is proportional to the diagonal element of the Wilson G-matrix,⁴² corresponding to the reaction coordinate.

(45) McQuarrie, D. A. *Statistical Mechanics*; Harper & Row: New York, 1976.

(46) Berne, B. J. In *Multiple Time Scales*; Brackbill, J. U., Cohen, B. I., Eds.; Academic: New York, 1985.

(29) Lim, C.; Tully, J. C. *J. Am. Chem. Soc.* **1984**, *106*, 5425.

(30) Northrup, S. H.; Hynes, J. T. *J. Chem. Phys.* **1978**, *69*, 5246.

(31) Northrup, S. H.; Hynes, J. T. *J. Chem. Phys.* **1980**, *73*, 2700.

(32) Caldeira, A. O.; Leggett, A. J. *Ann. Phys. (New York)* **1983**, *149*, 374.

(33) Pollak, E. *Phys. Rev. A* **1986**, *33*, 4244.

(34) Wigner, E. J. *Chem. Phys.* **1937**, *5*, 720.

(35) Eyring, H. *J. Chem. Phys.* **1934**, *3*, 107.

(36) Callear, A. B. *Comprehensive Chemical Kinetics, Modern Methods in Kinetics*; Elsevier: New York, 1983; Vol. 24, p 333.

(37) Reinhardt, W. P. *J. Phys. Chem.* **1982**, *86*, 2158.

bimolecular reaction (2.6) is inversely proportional to the volume of the system and will vanish in the thermodynamic limit. In this case we are interested in a bimolecular rate constant which has units of volume per unit time. This quantity is obtained by multiplying (2.6) by the volume of the system before taking the thermodynamic limit of infinite volume.⁴⁷

The central quantity which determines the transition-state rate constant in a solvent is the potential of mean force as a function of the reaction coordinate.^{15,45} It can be evaluated in either Monte Carlo⁴⁸ or molecular dynamics simulations⁴⁹ by determining the probability distribution of the reaction coordinate x .⁴⁶ However, regions near a high barrier will be sampled infrequently. To sample these portions of phase space more effectively, one employs umbrella sampling.⁴⁸⁻⁵⁰ This is done by choosing an umbrella potential $U_0(x)$ which roughly approximates the expected $W(x)$. One then studies the equilibrium properties of a modified system described by the potential energy surface $U(r) - U_0(x)$ using Monte Carlo or molecular dynamics. Again, a probability distribution of the reaction coordinate x is accumulated, but in this case it will be proportional to $e^{-\beta[W(x) - U_0(x)]}$. Therefore, all regions of coordinate space should be sampled with approximately equal efficiency. By dividing out the trial function, one obtains the potential of mean force $W(x)$.

Independent of the dividing surface, the canonical transition-state rate constant is always an upper bound to the true rate constant. The overall rate constant cannot depend on the choice of the dividing surface. However, the transition-state rate constant is sensitive to the choice of dividing surface and, for a dividing surface which minimizes the transition-state rate constant, might give an excellent approximation to the true rate constant. This is the spirit of variational transition-state theory.^{2,51}

How do we find such a dividing surface? This can be answered at different levels. If the reaction is described by a one-dimensional reaction coordinate moving in a potential of mean force arising from all remaining degrees of freedom,⁵² the best dividing surface will be located at the maximum of the potential of mean force. Obviously, for a polyatomic molecule a better choice might be some linear combination of all internal coordinates which would lead to a smaller rate constant and a better upper bound. Finally, one might want to consider a linear combination of all coordinates of the solvent and solute which will give the best possible transition-state theory. Recently, Pollak has shown that both Kramers and Grote-Hynes theory (see section 5) follow from such a multidimensional transition-state theory which includes all solvent degrees of freedom.⁵³ This gives rise to diffusion-controlled behavior and provides an interesting reinterpretation of the Lindemann mechanism (see section 1) where the high collision limit is treated by the multidimensional TST.⁵⁴

In the simplest case of an isolated single degree of freedom, $W(x) = U(x)$ and (2.6) gives

$$k_{\text{TST}} = (\omega_0/2\pi)e^{-\beta Q} \quad (2.8)$$

where ω_0 is the frequency in the well. Generalization to many degrees of freedom gives⁵⁵

$$k_{\text{TST}} = \frac{1}{2\pi} \frac{\prod_i \omega_i^{(0)}}{\prod_i \omega_i^{(s)}} e^{-\beta Q} \quad (2.9)$$

where $\omega_i^{(0)}$ and $\omega_i^{(s)}$ are the frequencies of the stable normal modes of the reactant minimum and saddle, respectively.

In the simplest realistic case of a diatomic molecule the reaction coordinate is $x = r - r_s$, the distribution function is $S(x) \propto r^2 e^{-\beta U(r)}$, and μ is the reduced mass. For an interaction potential that vanishes for $r > a$ and is strongly attractive for $r < a$ the dividing surface lies at $r_s = a$ and the bimolecular transition-state rate constant (2.6) becomes in the "free molecular limit"

$$k_{\text{TST}} = (8\pi/\mu\beta)^{1/2} a^2 \quad (2.10)$$

Note that we have dropped a factor of the volume of the system which results from the integral $\int dr r^2$.

In a diatomic molecule, $S(r) \propto r^2 e^{-\beta U(r)}$, which is equivalent to $e^{-\beta U_{\text{eff}}(r)}$, where $U_{\text{eff}}(r)$ is an effective potential consisting of the sum of the bare potential $U(r)$ and the centrifugal potential, $-2k_B T \log r$. In the general case, the effective potential is $U_{\text{eff}}(r) = U(r) - k_B T \log J$, where J is the Jacobian of the transformation from lab frame to internal molecular frame. For example, in a triatomic molecule $J \propto r^2 s^2 \sin \theta$, where r and s are the two bond lengths and θ is the angle between them.⁵⁶ In this case, (2.9) will always apply using this modified potential. For a bimolecular reaction, (2.9) will be slightly modified as the potential of mean force will give a factor of the volume of the system.

The foregoing applies only to an isolated molecule. If the molecule is inserted into a solvent, $S(x)$ will be modified.¹⁵ Again, consider the diatomic as an example. In this case, $S(r) \propto r^2 g(r)$, where $g(r)$ is the pair distribution function which is conveniently written as $g(r) = y(r)e^{-\beta U(r)} = e^{-\beta[U(r) + W(r)]}$, where $y(r)$ is the cavity distribution function and $W(r)$ is the potential of mean force induced by the solvent. At zero pressure, $y(r) = 1$ and $W(r) = 0$. Neglecting the small variation of the frequencies and the dividing surface, the rate constant becomes

$$k_{\text{TST}} \approx \frac{y(r_s)}{y(r_0)} \frac{\omega_0}{2\pi} e^{-\beta Q} \quad (2.11)$$

which is now density dependent because of the density dependence of $y(r)$.

At low pressures, or densities, it is possible to perform a virial expansion so that the variation of k_{TST} as a function of density is characterized by constant reaction volume

$$\frac{\partial \ln k_{\text{TST}}}{\partial \rho} = -\Delta V_{\text{TST}} \quad (2.12)$$

at low densities. At low densities for hard sphere solvent-solute interactions ΔV_{TST} is the excluded volume difference between the molecule confined to the transition state and the reactant. This is related to the fact that the second virial coefficient is half the excluded volume of the solute for hard sphere interactions.⁴⁵ In this context, the old intuitive concept of the "reaction volume" arises as a special case of a microscopic theory. At higher densities k_{TST} will no longer vary linearly with the density and the reaction volume will no longer be a constant. Such concepts are easily generalized to more complicated molecules. However, the determination of a multidimensional potential of mean force is difficult. The more practical approach is the consideration of a one-dimensional reaction coordinate where the potential of mean force can be estimated by umbrella sampling techniques.

As mentioned earlier, in practice the assumptions of transition-state theory may not be met. In particular, the first assumption of a steady-state distribution of reactant states may be violated by dynamic effects such as ineffective energy activation. Additionally, the manifold of activated states may not be ergodic so that less than the full measure of reactant states can access the transition-state region. The second assumption, that activated reactant states will cross the transition state and be deactivated with certainty, may be violated if activated reactants recross the transition-state surface before deactivation. In the next section we will discuss numerical methods for calculating dynamic, and nonergodic, corrections to transition-state theory.

(47) Unimolecular reactions have been analyzed carefully within the reactive flux formalism.⁴¹ While an analogous study is lacking for bimolecular reactions, we believe all the expressions apply to the bimolecular case.⁴³

(48) Rosenberg, R. O.; Mikkilineni, R.; Berne, B. J. *J. Am. Chem. Soc.* **1982**, *104*, 7647.

(49) Rebertus, D. W.; Berne, B. J.; Chandler, D. *J. Chem. Phys.* **1979**, *70*, 3395.

(50) Valleau, J. P.; Whittington, S. G. In *Statistical Mechanics, Part A*; Berne, B. J., Ed.; Plenum: New York, 1976.

(51) Keck, J. C. *Adv. Chem. Phys.* **1967**, *13*, 85.

(52) Miller, W. H. *J. Chem. Phys.* **1974**, *61*, 1923.

(53) Pollak, E. *J. Chem. Phys.* **1986**, *85*, 865.

(54) In this case, the connection formula (6.2) follows directly.

(55) Slater, N. B. *Theory of Unimolecular Reactions*; Cornell University Press: Ithaca, NY, 1959.

(56) Rodger, P. M.; Sceats, M. G. *J. Chem. Phys.* **1985**, *83*, 3358.

3. Numerical Methods

For barrier height $Q \gg k_B T$, numerical calculation of rate constants is difficult because the barrier-crossing events are extremely infrequent. This causes a separation of time scales in the system, between the time for energy activation and free motion in the potential, of order $e^{\beta Q}$. The calculation is so computationally intensive that it is virtually impossible to follow numerically a reacting system over several reactive events. Nonetheless, methods based on the reactive flux formalism^{41,8,51,57-59} circumvent this difficulty by starting trajectories on the top of the barrier, therefore sampling only activated events. They offer simple and practical methods for calculating rate constants in complex systems with good accuracy.⁴⁶

One must first define a physically meaningful reaction coordinate x which may be a bond length or a bond angle. In general, it is a function of the configurational coordinates $\mathbf{r} (r_1, \dots, r_{3N})$. It is zero at the transition-state dividing surface which is located at or near the saddle point \mathbf{r}_s . The actual value of the rate constant will be independent of the choice of the reaction coordinate and the location of the dividing surface. However, to achieve maximum computational efficiency, it should be placed close to the top of the barrier.

The calculation of the true kinetic rate constant $k = k_f + k_b$ can be conveniently expressed in terms of two separate tasks, namely, a calculation of the kinetic transition-state rate constant $k_{\text{TST}} = k_{\text{TST}}^f + k_{\text{TST}}^b$ and a calculation of the transmission coefficient κ

$$k = \kappa k_{\text{TST}} \quad (3.1)$$

Similar expressions are valid for the forward and backward rate constants;

$$k_f = \kappa k_{\text{TST}}^f \quad (3.2)$$

$$k_b = \kappa k_{\text{TST}}^b \quad (3.3)$$

The rate constant given by transition-state theory must be evaluated separately for the forward reaction and the backward reaction as described in section 2. The transmission coefficient κ is the same for the forward as well as the backward reaction. Note that whereas k_{TST} and κ depend on the choice of reaction coordinate x , their sum, i.e., the overall rate constant k , is independent of this choice. Detailed balance relates the ratio of the forward rate and backward rate to the equilibrium constant.

The transmission coefficient κ , which is a dynamic quantity, is related to the normalized reactive flux^{41,46}

$$\hat{k}(t) = \frac{\langle \delta(x) \dot{x} \theta(x(t)) \rangle}{\langle \delta(x) \dot{x} \theta(\dot{x}) \rangle} \quad (3.4)$$

where the quantities without a time variable are taken at the time origin, e.g., $x = x(0)$. An example of this function, obtained from a simulation, is plotted in Figure 5; the normalized reactive flux starts at 1 and decays to a plateau value which is the transmission coefficient κ . For a unimolecular reaction the plateau decays very slowly in time whereas for an atom-transfer reaction it converges to a true plateau. In either case, the relevant transmission coefficient κ entering (3.1) can be obtained by extrapolating the plateau of $\hat{k}(t)$ to zero time (see Figure 5).

A practical expression for evaluating $\hat{k}(t)$ numerically is obtained by inserting $\theta(\dot{x}) + \theta(-\dot{x}) = 1$ in the numerator of (3.4) which yields^{7,8,46}

$$\hat{k}(t) = \langle \theta(x(t))_+ - \theta(x(t))_- \rangle \quad (3.5)$$

where

$$\langle \dots \rangle_{\pm} = \frac{\langle \delta(x) \dot{x} \theta(\pm \dot{x}) \dots \rangle}{\langle \delta(x) \dot{x} \theta(\pm \dot{x}) \rangle} \quad (3.6)$$

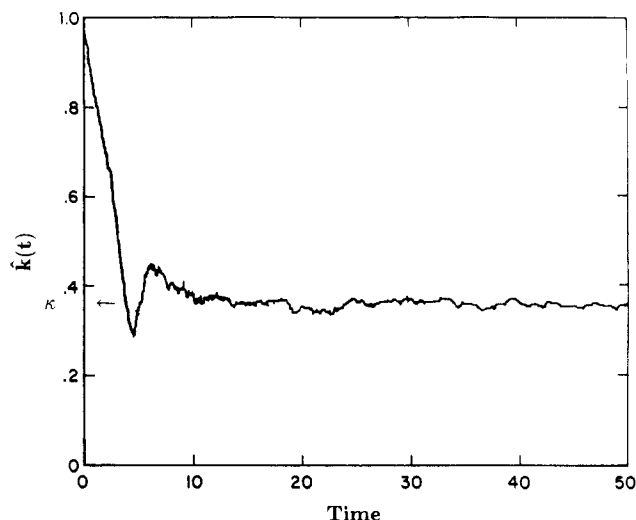


Figure 5. Typical reactive flux $\hat{k}(t)$ obtained from a numerical simulation, as a function of time. The oscillations at short time are due to transient recrossings, and the long time limit gives the plateau value which is the transmission coefficient κ .

is an average over a modified equilibrium distribution of initial conditions. These initial conditions are obtained by Monte Carlo sampling in position as well as velocity space from the distribution $\dot{x} e^{-\beta H}$, with frozen reaction coordinate $x = 0$, accepting only positive \dot{x} for averaging over $\langle \dots \rangle_+$ and negative \dot{x} for averaging over $\langle \dots \rangle_-$. In practice, one samples a set of $\dot{x} > 0$ to compute $\langle \theta \rangle_+$ and then uses the negative of this set for the computation of $\langle \theta \rangle_-$. For each set of initial conditions a trajectory is generated by using a molecular dynamics⁶⁰ or stochastic dynamics^{61,62} procedure and the average of $\theta[x(t)]$ is accumulated. Typically 10^2 – 10^4 independent trajectories are needed and, except for symmetric potentials, two calculations are performed to obtain $\langle \theta(x(t))_+ \rangle$ and $\langle \theta(x(t))_- \rangle$. Equation 3.5 gives the normalized reactive flux $\hat{k}(t)$ which will approach a plateau for longer times. In practice, it is absolutely essential to observe a plateau for at least 1 order of magnitude in time in order to establish that it is a true plateau. Shorter "plateaus" are likely to grossly overestimate the rate constant. It is also important that the initial conditions generated by the Monte Carlo procedure are uncorrelated. This is particularly difficult when studying reactions in slowly relaxing solvents, e.g., water.

The *full reactive flux method* has been used to calculate dynamic corrections to transition-state theory for thermal desorption from rare gas surfaces,⁶³ isomerization reactions in liquids using stochastic BKG^{8,9} and Newtonian⁶⁴ dynamics, as well as systems of biological interest such as ion pair formation and dissociation in water⁶⁵ and oxygen binding to myoglobin.⁶⁶ This method is practical if the transmission coefficient κ is not much smaller than unity. Unfortunately, calculations become prohibitively time consuming when κ is small since one must estimate a small difference in two numbers which are approximately unity. An essentially equivalent approach was used by Bergsma et al. to calculate rate constants for atom-transfer reactions.^{67,68}

To overcome this serious drawback we have recently developed an approximate version of this method—the *absorbing boundary method*—which enormously accelerates the calculation of rate

(60) Kushick, J.; Berne, B. J. In *Statistical Mechanics, Part B*; Berne, B. J., Ed.; Plenum: New York, 1976.

(61) Turq, P.; Lantelme, F.; Friedman, H. L. *J. Chem. Phys.* **1977**, *66*, 3039.

(62) Allen, M. P. *Mol. Phys.* **1980**, *40*, 1073.

(63) Adams, J. E.; Doll, J. D. *J. Chem. Phys.* **1984**, *80*, 1681.

(64) Rosenberg, R. O.; Berne, B. J.; Chandler, D. *Chem. Phys. Lett.* **1980**, *75*, 162.

(65) Karim, O. A.; McCammon, J. A. *Chem. Phys. Lett.* **1986**, *132*, 219.

(66) Case, D.; McCammon, J. A. *Ann. N.Y. Acad. Sci.*, in press.

(67) Bergsma, J. P.; Reimers, J. R.; Wilson, K. R.; Hynes, J. T. *J. Chem. Phys.* **1986**, *85*, 5625.

(68) Bergsma, J. P.; Gertner, B. J.; Wilson, K. R.; Hynes, J. T. *J. Chem. Phys.* **1987**, *86*, 1356.

(57) Yamamoto, T. *J. Chem. Phys.* **1960**, *33*, 281.

(58) Anderson, J. B. *J. Chem. Phys.* **1973**, *58*, 4684.

(59) Bennett, C. H. In *Algorithms for Chemical Computation*; Christoferson, R. E., Ed.; American Chemical Society: Washington, DC, 1977.

constants and makes accurate calculation of small transmission coefficients possible.^{69,70} The accuracy of this method rests on a single, apparently excellent, assumption: trajectories which recross the transition-state conform to the distribution $\bar{x}e^{-\beta H}$. The quantities required are two survival probabilities

$$P_{\pm}(t) = \langle \theta'(\pm x(t)) \rangle_{\pm} \quad (3.7)$$

where $P_{\pm}(t)$ measures the number of trajectories which have not recrossed the transition state. $\theta'(\pm x(t))$ is unity until the trajectory crosses the transition state and zero thereafter. The survival probabilities $P_{\pm}(t)$ will start at unity and monotonically decrease to a slowly decaying plateau as for $\bar{k}(t)$.

The Laplace transform of the reactive flux $\bar{k}(s)$ is related to the Laplace transforms of the survival probabilities $\bar{P}_{\pm}(s)$ by⁷⁰

$$\bar{k}(s) \simeq \frac{\bar{P}_+(s)\bar{P}_-(s)}{\bar{P}_+(s) + \bar{P}_-(s) - s\bar{P}_+(s)\bar{P}_-(s)} \quad (3.8)$$

If $P_{\pm}(t)$ approaches a plateau value T_{\pm} for long times, these quantities can be used to obtain the plateau value of the reactive flux, i.e., the transmission coefficient, using^{69,71}

$$\kappa \simeq \frac{T_+T_-}{T_+ + T_- - T_+T_-} \quad (3.9)$$

which follows from (3.8). In a symmetric potential, $P_+(t) = P_-(t)$ and $T_+ = T_-$ so that only one survival probability is needed. The same formula was proposed in a statistical theory for bimolecular reactions which form collisional complexes.⁷²

To obtain $P_{\pm}(t)$ one samples positions and velocities from $\bar{x}\theta(\bar{x})e^{-\beta H}$ with frozen $x = 0$ using Monte Carlo as in the full reactive flux calculation. For each set of initial conditions a trajectory is followed until it recrosses the transition state where it is removed. The average fraction of nonabsorbed trajectories gives the survival probability $P_+(t)$. The same calculation with negative \bar{x} gives $P_-(t)$. Trajectories will be followed until the true plateau of $P_{\pm}(t)$ is reached as in the *full reactive flux method*. The absorbing boundary method has been applied to one-dimensional systems with Markovian^{69,70} and non-Markovian^{73,74} weak collision friction models, and double well systems for both weak⁷⁵ and strong⁷⁶ collision models. It has proven especially useful and accurate in rate constant calculations for aqueous and biomolecular systems such as ion pair formation and dissociation in water,⁶⁵ and side-chain rotational isomerization in a solvated protein.⁷⁷ Whereas the absorbing boundary method resolves the problem of estimating small transmission coefficients, κ , one still has to integrate the equations of motion long enough to reach the plateau. This is not a problem for single and many degree of freedom systems at higher damping where the dynamics resembles a single degree of freedom (section 4.4). However, a strongly coupled many degree of freedom system which is weakly damped will take a very long time to reach the plateau and this can make calculations prohibitively expensive.

Diffusion-controlled reactions¹⁴ which involve the relative diffusion of reactant pairs, such as ion recombination and enzyme substrate reactions, can be studied with reactive flux methods using Langevin dynamics at high damping. However, a more effective method for calculating rate constants is the Brownian dynamics simulation method of Northrup et al.^{78,79} Here, the bimolecular

rate constant is conveniently expressed as a simple product

$$k = k(s) p(s,*) \quad (3.10)$$

where $k(s)$ is the rate at which reactants reach a separation $r = s$ and $p(s,*)$ is the fraction of reactant pairs, initially at $r = s$, which will react rather than diffuse to infinite separation. The basis of this method involves ideas quite similar to those used in the absorbing boundary method.⁷⁸ This method and extensions thereof have shown excellent agreement with analytic models for centrosymmetric potentials.^{80,81} It has also been applied to more realistic models of biological interest which include anisotropic electrostatic interactions.^{80,82}

In this section, we have discussed efficient numerical methods for calculating rate constants in complex systems. For reactions involving barrier crossing the calculation is conveniently split into a calculation of the transition-state rate constant and a calculation of the transmission coefficient. The transition-state rate constant is an equilibrium average and can be obtained from the potential of mean force. The transmission coefficient is a dynamical quantity which can be obtained from the plateau value of the reactive flux. Two related methods are available for the calculation of this quantity: the *full reactive flux method* and the *absorbing boundary method*. Whereas the *full reactive flux method* is exact, it tends to be costly in computer time; the approximate but accurate *absorbing boundary method* is much faster, is easier to program, and therefore is the method of choice. For problems involving the relative diffusion of two particles where the diffusion coefficients are very small, the Brownian dynamics method is most effective.

4. Unimolecular Rate Theory

The theory of unimolecular reactions in the gas phase has received much attention, and excellent reviews^{17,19} and monographs^{13,55} are available. This approach is based on the observation that at zero pressure the total energy of the molecule is a conserved variable. In a dilute gas the molecule will suffer infrequent collisions with the gas molecules. The energy will be slowly varying and will change in a jumpwise fashion. Since subsequent collisions are uncorrelated the evolution of the energy can be described by a simple rate equation.

If all other variables relax rapidly, the energy of n strongly coupled degrees of freedom, forming the reaction system, will equipartition rapidly on the energy shell. This is the assumption of rapid energy partitioning inherent in RRKM theory. The probability density $P(E,t)$ for finding a dissociating molecule with an energy E on the reactant side will then satisfy the master equation^{17,83}

$$\frac{\partial P(E,t)}{\partial t} = \int dE' [K(E,E')P(E',t) - K(E',E)P(E,t)] - k_{\text{RRKM}}(E)P(E,t) \quad (4.1)$$

The transition probability $K(E',E)$ obeys the detailed balance condition

$$K(E,E') P_{\text{eq}}(E') = K(E',E) P_{\text{eq}}(E) \quad (4.2)$$

where the thermal distribution of the energy

$$P_{\text{eq}}(E) \propto \Omega(E)e^{-\beta E} \quad (4.3)$$

(69) Straub, J. E.; Berne, B. J. *J. Chem. Phys.* **1985**, *83*, 1138.
 (70) Straub, J. E.; Hsu, D. A.; Berne, B. J. *J. Phys. Chem.* **1985**, *89*, 5188.
 (71) Glasstone, S.; Laidler, K. J.; Eyring, H. *The Theory of Rate Processes*; McGraw-Hill: New York, 1941.
 (72) Miller, W. H. *J. Chem. Phys.* **1976**, *65*, 2216.
 (73) Straub, J. E.; Borkovec, M.; Berne, B. J. *J. Chem. Phys.* **1985**, *83*, 3172.
 (74) Straub, J. E.; Borkovec, M.; Berne, B. J. *J. Chem. Phys.* **1986**, *84*, 1788. Addendum and Erratum, *Ibid.* **1986**, *86*, 1079.
 (75) Straub, J. E.; Berne, B. J. *J. Chem. Phys.* **1986**, *85*, 2999.
 (76) Borkovec, M.; Straub, J. E.; Berne, B. J. *J. Chem. Phys.* **1986**, *85*, 146.
 (77) Ghosh, I.; McCammon, J. A. *Biophys. J.* **1987**, *51*, 637.

(78) Northrup, S. H.; Allison, S. A.; McCammon, J. A. *J. Chem. Phys.* **1984**, *80*, 1517.
 (79) McCammon, J. A.; Northrup, S. H.; Allison, S. A. *J. Phys. Chem.* **1986**, *90*, 3901.
 (80) Allison, S. A.; Northrup, S. H.; McCammon, J. A. *J. Chem. Phys.* **1985**, *83*, 2894.
 (81) Northrup, S. H.; Curvin, M. S.; Allison, S. A.; McCammon, J. A. *J. Chem. Phys.* **1986**, *84*, 2196.
 (82) Northrup, S. H.; Smith, J. D.; Boles, J. O.; Reynolds, J. C. L. *J. Chem. Phys.* **1986**, *84*, 5536.
 (83) Borkovec, M.; Berne, B. J. *J. Chem. Phys.* **1985**, *82*, 794.

is the Boltzmann factor times the density of states

$$\Omega(E) = \int d\Gamma \delta[E - H(\Gamma)] \quad (4.4)$$

The integration over the spatial coordinates has to be restricted to the reactant region. For a collection of n harmonic oscillators one finds that $\Omega(E) \propto E^{n-1}$.

The transition probability density $K(E', E)$ is a collision rate α times the probability density $P(E', E)$ of the molecule having energy E' after the collision, given it had an energy E prior to the collision. Even though the collision rate depends on the energy of the molecule in general, it is often taken to be a constant. The integral term of (4.1) describes the change in the energy of the molecule due to collisions with molecules of the bath gas. The last term in (4.1) describes the loss of molecules due to dissociation. This process is approximated by RRKM theory (see section 2) where $k_{\text{RRKM}}(E)$ is the rate at which a molecule of given energy above the dissociation threshold dissociates. Note that $k_{\text{RRKM}}(E)$ vanishes for energies below the energy threshold Q . First we focus on dissociation reactions; recombination reaction rate constants are obtained by detailed balance. At the end of this section we discuss the extension of these ideas to isomerization reactions.

The calculation of the rate constant k from (4.1) is based on the observation that $P(E, t)$ will decay like $P_{\text{ss}}(E)e^{-kt}$ after an initial transient period. The steady-state distribution $P_{\text{ss}}(E)$ can be evaluated by inserting this *ansatz* into (4.1). Since the rate constant is very small, the left-hand side of (4.1) can be neglected and the resulting equation can be solved for the steady-state distribution $P_{\text{ss}}(E)$. The rate constant is then simply given by the total flux

$$k = \int dE P_{\text{ss}}(E) k_{\text{RRKM}}(E) \quad (4.5)$$

At high collision rate α the rate of energy activation is so rapid that $P_{\text{ss}}(E) = P_{\text{eq}}(E)$ above the dissociation threshold. In this case the overall rate constant is given by transition-state theory (cf. (2.4)), i.e.

$$k = k_{\text{TST}} \quad \text{for } \alpha \rightarrow \infty \quad (4.6)$$

On the other hand, as the collision rate approaches zero, the molecule will certainly dissociate before being deactivated and $P_{\text{ss}}(E) = 0$ for $E > Q$. In this case, (4.5) becomes indefinite and a more useful expression for the rate constant is derived from the steady-state flux

$$k = \int_0^\infty dE' \int_0^Q dE K(E', E) P_{\text{ss}}(E) \quad \text{for } \alpha \rightarrow 0 \quad (4.7)$$

The above treatment is entirely equivalent to other methods for calculating rate constants such as the mean first passage time approach,⁸⁴⁻⁸⁶ correlation functions,^{27,31,87} or analysis of the eigenvalue spectrum.⁸⁸

An important characteristic of a collision kernel is the energy transferred per unit time

$$A(E) = \int dE' K(E', E)(E' - E) = \alpha \langle \Delta E \rangle \quad (4.8)$$

or equivalently the average energy transferred per collision $\langle \Delta E \rangle$. If the energy transferred per collision is large compared with the thermal energy $\langle \Delta E \rangle \gg k_{\text{B}}T$, we have a *strong collision model*.^{1,13,17,38,89,90} In this case a single collision can change the energy of a molecule by a large amount and one collision is sufficient to activate a molecule above the dissociation threshold. On the other hand, if the energy change is small $\langle \Delta E \rangle \ll k_{\text{B}}T$, we have a *weak collision model*.^{1,13,17,90,91} Here the energy of a molecule

can change only by a small amount and many collisions are required to activate a molecule to the dissociation threshold. We shall discuss these two limiting cases first before we discuss the realistic intermediate case between these two limits.

4.1. Strong Collision Models ($\langle \Delta E \rangle \gg k_{\text{B}}T$). The most popular strong collision model is the *strong collision approximation* where¹³

$$K_{\text{SC}}(E', E) = \alpha P_{\text{eq}}(E) \quad (4.9)$$

In this case the collisions are very strong so they resample the total energy from a thermal ensemble. This collision kernel allows for large energy transfer per collision. In the *strong collision approximation* (4.1) can be solved and the rate constant becomes

$$k_{\text{SC}} = \int dE P_{\text{eq}}(E) \frac{\alpha k_{\text{RRKM}}(E)}{\alpha + k_{\text{RRKM}}(E)} \quad (4.10)$$

For high collision rates, the rate constant becomes

$$k_{\text{SC}} = \int_0^\infty dE P_{\text{eq}}(E) k_{\text{RRKM}}(E) = k_{\text{TST}} \quad \text{for } \alpha \rightarrow \infty \quad (4.11)$$

which is simply transition-state theory. On the other hand at low collision rates^{13,19}

$$k_{\text{SC}} = \alpha \int_0^\infty dE P_{\text{eq}}(E) = \alpha \langle \theta(Q - H) \rangle \quad \text{for } \alpha \rightarrow 0 \quad (4.12)$$

which is simply the collision rate times the probability that the molecule is above the dissociation threshold. Using a harmonic density of states for high barriers³⁸

$$k_{\text{SC}} = \alpha \frac{(\beta Q)^{n-1}}{(n-1)!} e^{-\beta Q} \quad \text{for } \alpha \rightarrow 0 \quad (4.13)$$

a result first derived by Hinshelwood.^{55,92} Different strong collision models, e.g., the BGK model,^{8,93-95} can be devised. However, the rate constant is always well approximated by the *strong collision approximation*.

4.2. Weak Collision Models ($\langle \Delta E \rangle \ll k_{\text{B}}T$). Let us consider the *weak collision approximation* where the energy changes upon collision are assumed to be so small that the motion in the energy shell is equivalent to a small step diffusion process. In this case we can perform a Kramers-Moyal expansion of (4.1) which gives⁸³

$$\frac{\partial P(E, t)}{\partial t} = -\frac{\partial}{\partial E} [A(E)P(E, t)] + \frac{\partial^2}{\partial E^2} [D(E)P(E, t)] - k_{\text{RRKM}}(E)P(E, t) \quad (4.14)$$

where the energy diffusion coefficient

$$D(E) = \frac{1}{2} \int dE' K(E', E)(E' - E)^2 \quad (4.15)$$

is related to the energy transferred per unit time by

$$A(E) = \frac{1}{P_{\text{eq}}(E)} \frac{d}{dE} [D(E)P_{\text{eq}}(E)] \quad (4.16)$$

This relation follows from the detailed balance condition (4.2).

Unfortunately, the complete calculation of the rate constant is difficult. An analytic solution is feasible in the low collision limit which gives

$$k_{\text{WC}} = \left[\int_0^Q dE \frac{1}{D(E)P_{\text{eq}}(E)} \int_0^E dE' P_{\text{eq}}(E') \right]^{-1} \quad (4.17)$$

(84) Montroll, E. W.; Shuler, K. E. *Adv. Chem. Phys.* **1958**, *1*, 361.

(85) Gardiner, C. W. *Handbook of Stochastic Methods*; Springer: New York, 1983.

(86) Knessel, C.; Mangel, M.; Matkowsky, B. J.; Schuss, Z.; Tier, C. J. *Chem. Phys.* **1984**, *81*, 1285.

(87) Grote, R. F.; Hynes, J. T. *J. Chem. Phys.* **1980**, *73*, 2715.

(88) Widom, B. *J. Chem. Phys.* **1971**, *55*, 44.

(89) Troe, J. *J. Chem. Phys.* **1977**, *66*, 4758.

(90) Skinner, J. L.; Wolynes, P. G. *J. Chem. Phys.* **1980**, *72*, 4913.

(91) Troe, J. *J. Chem. Phys.* **1977**, *66*, 4745.

(92) Hinshelwood, C. N. *The Kinetics of Chemical Change in Gaseous Systems*; Clarendon Press: Oxford, 1933.

(93) Bhatnagar, P. L.; Gross, E. P.; Krook, R. M. *Phys. Rev.* **1954**, *94*, 511.

(94) Skinner, J. L.; Wolynes, P. G. *J. Chem. Phys.* **1978**, *69*, 2143.

(95) Berne, B. J.; Skinner, J. L.; Wolynes, P. G. *J. Chem. Phys.* **1980**, *73*, 4314.

a result first derived by Kramers.^{1,85} It is convenient to introduce a collision efficiency β_c which is the rate constant of a given collisional model relative to the *strong collision approximation*.⁸⁹ For the weak collision model the collision efficiency can be shown to be⁸⁹

$$\beta_c \simeq -\beta \langle \Delta E \rangle \simeq \beta^2 D(Q) / \alpha \quad (4.18)$$

which is correct in the high barrier limit. To make contact with Kramers' work, consider a collection of strongly coupled damped degrees of freedom. In this case the energy diffusion coefficient becomes

$$D(E) = \sum_{ij} (\zeta_{ij} / m_i m_j) \langle v_i v_j \rangle_E \quad (4.19)$$

where ζ_{ij} are the elements of the friction tensor, m_i are the masses of the particles, and $\langle \dots \rangle_E$ is the microcanonical average. This result has been derived by Kramers for $n = 1$,¹ and we have recently obtained the general result for arbitrary n .⁸³ For a collection of n harmonic oscillators with isotropic mass and friction

$$D(E) = (\zeta / m) k_B T E \quad (4.20)$$

Inserting this into (4.17) and using (4.3), we obtain^{83,96,97}

$$k_{WC} = \frac{\zeta}{m} \frac{(\beta Q)^n}{(n-1)!} e^{-\beta Q} \quad (4.21)$$

which is the low friction Kramers rate constant applicable to an arbitrary number of degrees of freedom.⁹⁸ This argument can be extended to a time-dependent friction kernel (non-Markovian). Now the energy diffusion coefficient becomes^{99,100}

$$D(E) = \sum_{ij} \int_0^\infty dt (\zeta_{ij}(t) / m_i m_j) \langle v_i(0) v_j(t) \rangle_E \quad (4.22)$$

The physical reason for a frequency-dependent friction kernel at low collision rate is the finite duration of a soft collision. Instantaneous hard sphere collisions with a heavy reactant give rise to a frequency-independent Markovian friction kernel. In general, a slowly decaying friction kernel will reduce the energy diffusion coefficient and thereby the energy activation rate.²⁷ This is a consequence of realistic soft collisions reducing the VT-energy transfer rate enormously. On the other hand, an oscillatory friction kernel will follow from a VV-transfer process which will increase the energy transfer rate and thereby the rate constant.

Solution of (4.14) for arbitrary ζ is not feasible except in the case of $n = 1$ ¹⁰¹ and $n = 2$.¹⁰² The corrections to the low friction weak collision result can be evaluated for general n .¹⁰² The rate constant relative to the transition-state theory result k_{TST} is given by

$$k/k_{TST} = z(1 - \text{const } z^{1/(n+1)} + \dots) \quad (4.23)$$

where $z = k_{WC}/k_{TST}$. With increasing n , the correction terms become increasingly important and cannot be neglected for most applications for $n \geq 2$.¹⁰³

4.3. Between Weak and Strong Collisions. The transition between the strong collision model and the weak collision model has been studied in much detail by Troe.^{17,89,91} One model where the rate constant can be evaluated analytically^{89,91,104} is the ex-

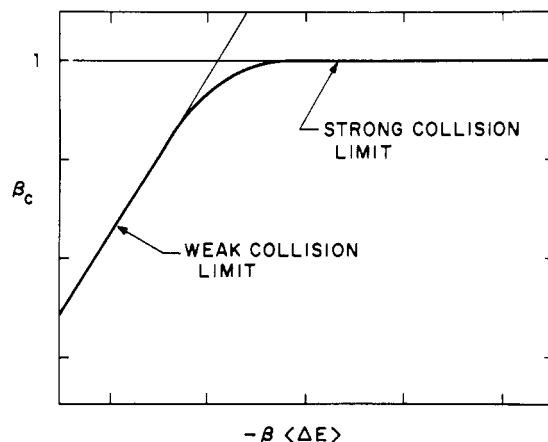


Figure 6. Schematic log-log plot of the transition between the weak and strong collision limits. The collision efficiency, β_c , is plotted as a function of the average energy transfer per collision, $\langle \Delta E \rangle$.

ponential model where one assumes the following form for the collision kernel⁹¹

$$K(E', E) = \frac{\alpha}{a+b} e^{-|E'-E|/a} \quad \text{for activation } E' > E$$

$$K(E', E) = \frac{\alpha}{a+b} e^{-|E'-E|/b} \quad \text{for deactivation } E > E' \quad (4.24)$$

The collision efficiency β_c is determined by the implicit relation⁹¹

$$\frac{\beta_c}{1 - \beta_c^{1/2}} = - \frac{\langle \Delta E \rangle}{k_B T} \quad (4.25)$$

from $\langle \Delta E \rangle$. This expression gives the strong collision approximation $\beta_c = 1$ for $|\langle \Delta E \rangle| \gg k_B T$ and approaches the weak collision or energy diffusion limit for $|\langle \Delta E \rangle| \ll k_B T$ (see Figure 6). Different collision kernels have been studied numerically^{90,91} with the result that (4.24) applies approximately for many realistic collision kernels. Equivalent results have been obtained using mean first passage time techniques.¹⁰⁵

4.4. Extension to Slow IVR. All models discussed so far are based on the following two assumptions about the internal dynamics of the molecule: first, rapid and complete energy equipartitioning on the energy shell and, second, the validity of microcanonical transition-state theory. These assumptions may not be met.^{18,19} Suppose that we have some high-frequency modes in our molecule which might be very weakly coupled to the low-frequency reactive mode. We have recently presented the solution of this problem in the *strong collision approximation* without making *any* assumptions about the internal dynamics of the molecule. The rate constant becomes⁷⁶

$$k_{SC}/k_{TST} = \alpha \int_0^\infty dt e^{-\alpha t} k^{(0)}(t) \quad (4.26)$$

where $k^{(0)}(t)$ is the normalized reactive flux of the isolated molecule.¹⁰⁶

One can easily verify³⁸ that this expression reduces to (4.12) if the dynamics of the isolated molecule is described by RRKM theory having a reactive flux

$$k^{(0)}(t) = \langle k_{RRKM}(E) e^{-k_{RRKM}(E)t} \rangle / k_{TST} \quad (4.27)$$

where the thermal average is taken over the whole phase space.

In general, at high collision rates the reactive flux can be replaced by unity and the rate constant approaches transition-state theory. At low collision rates we have

(104) Penner, A. P.; Forst, W. *J. Chem. Phys.* **1977**, *67*, 5296.

(105) Knessel, C.; Matkowsky, B. J.; Schuss, Z.; Tier, C. *J. Stat. Phys.* **1985**, *42*, 169.

(106) This expression is probably entirely general and applies even to bimolecular atom-transfer reactions.⁴³

(96) Nitzan, A. *J. Chem. Phys.* **1985**, *82*, 1614.

(97) Matkowsky, B. J.; Schuss, Z. *SIAM J. Appl. Math.* **1982**, *42*, 835.

(98) Nitzan has presented a similar but incorrect result.⁹⁶ It is based on a different choice for the energy threshold. Simulations for a two degree of freedom system show clearly that (4.21) is the correct result.¹⁰³

(99) Zawadzki, A. G.; Hynes, J. T. *Chem. Phys. Lett.* **1985**, *113*, 476.

(100) Zwanzig, R. *Phys. Fluids* **1959**, *2*, 12.

(101) Büttiker, M.; Harris, E. P.; Landauer, R. *Phys. Rev. B: Condens. Matter* **1983**, *28*, 1268.

(102) Borkovec, M.; Berne, B. J. *J. Chem. Phys.* **1987**, *86*, 2444.

(103) Straub, J. E.; Borkovec, M.; Berne, B. J. *J. Chem. Phys.* **1987**, *86*, 4296.

$$k_{SC} = \alpha \int_0^{\infty} dt k^{(0)}(t) = \alpha \langle \theta_{cross} \rangle$$

$$= \alpha X^\dagger \int_Q^{\infty} dE P_{eq}(E) \quad \text{for } \alpha \rightarrow 0 \quad (4.28)$$

The characteristic function of phase space θ_{cross} is unity if a trajectory started at a particular phase point will eventually cross the transition state. X^\dagger is the measure of irregular phase space which is unity in the case of statistical energy partitioning and decreases as the surface becomes less ergodic.²⁰⁻²² If the trajectory is trapped on the reactant side, θ_{cross} vanishes. In the case of complete statistical energy partitioning $\theta_{cross} = \theta(Q - H)$, $X^\dagger = 1$, and (4.28) reduces to (4.12).

For intermediate intramolecular mode coupling the following physical picture emerges.^{18,19,75,76} At low collision frequency the system behaves like a strongly coupled system obeying RRKM theory and the rate constant rises rapidly with collision rate. At higher collision rates the system behaves rather like a single degree of freedom system and the rate constant rises more slowly with collision rate. This can be rationalized in terms of an intrinsic IVR rate which is the rate constant for energy exchange between the vibrational degrees of freedom. If the collision rate is smaller than the IVR rate, the activated molecule has time to explore the whole energy shell and can therefore dissociate before the next collision can deactivate it. If the collision rate is higher than the IVR rate and the activated molecule happened to have most of its energy in the nonreactive mode, it will have no time to transfer this energy into the reactive mode. The next collision will then certainly deactivate the molecule back into the reactant well. Put differently, for mean collision times longer than the inverse IVR rate (small collision rates) the reaction coordinate can lose its activation energy to the intramolecular modes between collisions and can thus appear to be multidimensional; whereas, for mean collision times shorter than the inverse IVR rate (large collision rates) the reaction coordinate will quickly lose its energy of activation to the bath instead of to the intramolecular modes and thus appear to be one-dimensional. Such non-RRKM effects are more important for larger molecules. Simulation data presented in Figure 7a illustrate this behavior.

If these non-RRKM effects are important in real molecules, measurements of the rate constant as a function of pressure should show a rapid rise initially which goes through a plateau and then rises more slowly as though having reduced dimensionality. Our studies on model systems have shown that such transitions from a rapid to a slower rise are probably smooth and stretch over several orders of magnitude of pressure. In cyclohexane there seems to be the expected rapid rise at lower pressures¹⁰⁷ changing into a slower rise at higher pressures.¹⁰⁸ Recent BGK simulations^{109,110} of cyclohexane are completely consistent with our point of view (see section 7).

In general $k^{(0)}(t)$ can be obtained from a simple trajectory calculation on the potential surface of the molecule in question. One starts trajectories as in a reactive flux calculation but follows the dynamics as in an isolated molecule. This procedure will give $k^{(0)}(t)$.⁷⁶ The absorbing boundary method^{69,70} will greatly accelerate the calculation. The ability of the surface to equipartition energy can be very easily estimated by comparing $\int_0^{\infty} dt k^{(0)}(t)$ with the RRKM prediction. We have applied this method to model problems with success.⁷⁶ It seems to be a very promising way to calculate rate constants in the *strong collision approximation* incorporating the proper dynamics of the isolated molecule. Very similar ideas have been used in chemical activation studies;¹⁹ the approach presented here allows us to compare results of such calculations with thermal data. Extension of this analysis for more

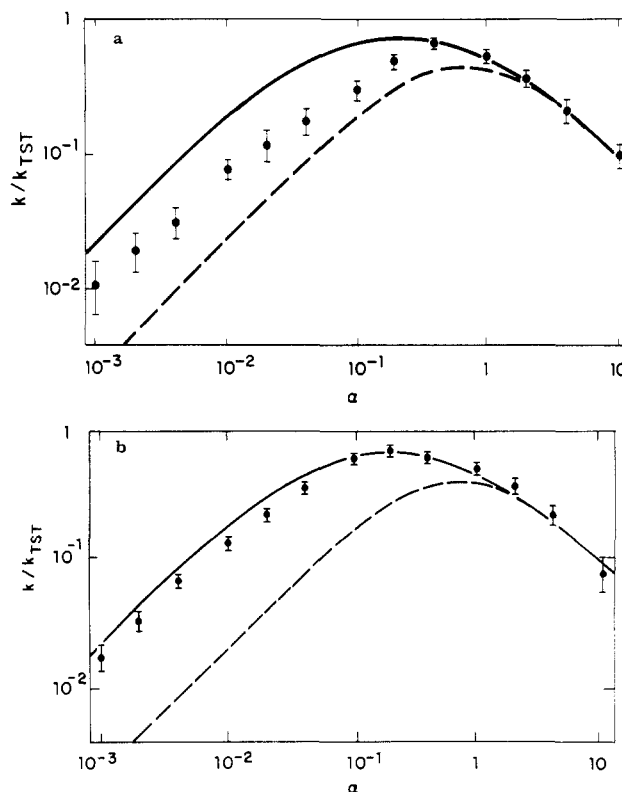


Figure 7. Log-log plot of the rate constant as a function of the collision frequency α for the BGK model using a two degree of freedom potential with both (a) intermediate and (b) strong coupling between degrees of freedom. Displayed are the predictions of the one-dimensional energy activation theory (---) and the RRKM theory (—), using (4.13) and (6.1) for $n = 1$ and 2, respectively, alongside numerical simulation results.⁷⁶

general collisional models^{75,103} would be highly desirable.

We have presented a numerical study of the transition between a strongly coupled system and a weakly coupled system using the strong collision approximation and the BGK model.⁷⁶ We have also studied a weak collision model in the intermediate coupling regime.⁷⁵ The behavior seems to be quite similar to the strong collision model.¹⁰³ It is unclear how important such effects are in real molecules.

4.5. Extension to Slow Angular Momentum Relaxation. Another simplification inherent in the present treatment is the fact that the total energy is the only slow variable. However, the angular momentum is also conserved in the isolated molecule. Therefore, at low collision rates in addition to the total energy the angular momentum will be a slowly relaxing variable which should be included in the master equation (4.1).^{19,91} The evaluation of rate constants is similar to the case of the energy being a slow variable. The main difference springs from the fact that the dissociation energy threshold will depend on the angular momentum of the molecule. In complete analogy with the previous analysis, the strong collision result is¹⁹

$$k_{SC} = \int dE dJ P_{eq}(E, J) \frac{\alpha k_{RRKM}(E, J)}{\alpha + k_{RRKM}(E, J)} \quad (4.29)$$

Again $k_{RRKM}(E, J)$ vanishes below the dissociation threshold. In general, the rate constants tend to be larger than for the one-dimensional method.

The study of the weak collision limit is more difficult. Nevertheless, some progress has been made. We have recently evaluated the rate constant using the coupled energy-angular momentum diffusion equation.¹¹¹ This approach takes the full coupling between angular momentum and energy relaxation into account. Application to a diatomic molecule gives the result

(107) Ross, B. D.; True, N. S. *J. Am. Chem. Soc.* **1983**, *105*, 1382. *Ibid.* **1983**, *105*, 4871.

(108) Hasha, D. L.; Eguchi, T.; Jonas, J. *J. Am. Chem. Soc.* **1982**, *104*, 2290.

(109) Kuharski, R. A.; Chandler, D.; Montgomery, J. A., Jr.; Rabii, F.; Singer, S. J. *J. Phys. Chem.*, in press.

(110) Chandler, D.; Kuharski, R. A., submitted for publication in *Faraday Discuss. Chem. Soc.*

(111) Borkovec, M.; Berne, B. J. *J. Chem. Phys.* **1986**, *84*, 4327.

$$k_{\text{WC}} = \int_0^{J_c} dJ P_{\text{eq}}(E, J) \left[D_{EE} - \frac{dQ}{dJ} D_{EJ} \right]_{E=Q(J)} \quad (4.30)$$

which reduces to (4.17) when the dissociation threshold is independent of the angular momentum. This result is equivalent to the treatment of Matkowsky et al.^{86,97,112} and is also very similar to the weak collision limit of Troe's solution of the exponential model in two dimensions.⁹¹ His solution is not limited to the weak collision limit but allows arbitrary $\langle \Delta E \rangle$ and $\langle \Delta J \rangle$.

Recently, Sceats suggested an interesting but somewhat ad hoc approach to this problem.¹¹³ He replaces the rotational effects by an effective potential of mean force (cf. section 2). Even though it is unclear why the dynamics could be described by such a potential at low collision rates, where the energy and angular momenta relax slowly, some preliminary results on the diatomic molecule look encouraging. Similar problems for polyatomic molecules should be addressed. Extended computer simulation of collision dynamics of a molecule in a low-pressure gas has helped to resolve these questions.^{114,115} Actually, we found¹¹⁶ that a simple molecular dynamics simulation at low pressure is much simpler to carry out than such a scattering calculation which requires averaging over a vast number of initial conditions.

4.6. Isomerization Reactions. Let us briefly discuss how these ideas extend to isomerization reactions. In general, (4.1) must be replaced with two coupled master equations where we consider activation and deactivation of the reactant as well as the product. This is rarely studied in detail. Again, in the high collision regime, transition-state theory will apply. In the low collision regime activation of the reactants will be rate limiting. However, once a particle is activated, there will be a finite probability that it will be deactivated into the product well. For example, in the case of a symmetric double well potential an activated trajectory will get trapped in either well with equal probability. Therefore, the low collision forward rate constant will be the energy activation rate reduced by a factor of $1/2$. In general, the trapping probability p can be evaluated from detailed balance. The forward rate constant is the rate constant for activation in the reactant well times p , and the backward rate constant is the rate constant for activation in the product well times $1 - p$. The ratio of the forward and backward rate constants is the equilibrium constant of the reaction. Therefore, the equilibrium constant determines the trapping probability p . It is interesting to note that in a polyatomic molecule the trapping probability in the deeper well can be quite substantial.

5. Diffusion-Controlled Reactions

If the collision frequency or friction coefficient is high, an activated reactant molecule will suffer frequent momentum-reversing collisions and recross the transition-state surface many times before being deactivated. In this case, the true rate constant will differ substantially from the transition-state theory rate constant. These deviations are treated by the theory of diffusion-controlled reactions.

The pioneering work in this field was done by Smoluchowski,^{14,28} who assumed that the spatial coordinate was slowly varying and the motion of the reaction coordinate could be described by

$$\frac{\partial p(x, t)}{\partial t} = D \frac{\partial}{\partial x} \left[\beta \frac{\partial U(x)}{\partial x} + \frac{\partial}{\partial x} \right] p(x, t) \quad (5.1)$$

where $p(x, t)$ is the probability density for finding the reaction coordinate at position x at time t , $U(x)$ is the potential felt by x , $\beta = 1/k_B T$, and D is the diffusion coefficient which is related to the static friction constant per unit mass or equivalently the

damping rate γ , the reduced mass of the reaction coordinate μ , and the temperature by $D = \mu k_B T / \gamma$. This is the Smoluchowski equation which describes the time evolution of a particle probabilistically.⁸⁵ The motion of the particle is assumed to be continuous in time as well as Markovian, so that the particle is completely described by its present position, independent of its history. For a solvated molecule this would demand that all collisions with solvent atoms be uncorrelated or that the force due to the solvent relax instantaneously.

We will consider two simple and important examples. First, a useful model for recombination reactions and reactions of ligand binding with enzymes is that of a particle diffusing in a centrally symmetric potential $U(r)$, where r is the reaction coordinate representing the interparticle separation of the reacting species. If it is assumed that the particles will react with probability unity when they reach a separation $r = a$, using the steady-state solution of (5.1) constant for a spherical potential, $U(r)$, it follows that

$$k_{\text{SD}} = 4\pi D \left[\int_a^\infty dr (e^{\beta U(r)} / r^2) \right]^{-1} \quad (5.2)$$

and taking $U(r) = 0$ results in²⁸

$$k = 4\pi D a \quad (5.3)$$

This is the famous Smoluchowski result which was generalized by Onsager and then Debye for ionic recombination^{117,118} and more recently by Northrup and Hynes for position-dependent diffusion.^{4,119} Corrections to the diffusion equation for moderate damping and corresponding corrections to the rate constant have been calculated by Skinner and Wolynes.¹²⁰

Second, for isomerization reactions in a bistable potential the rate constant for diffusion from the reactant well at x_0 to the product well at x_1 is given in analogy to (5.2)⁸⁵

$$k_{\text{SD}} = D \left[\int_{x_0}^{x_1} dx e^{\beta U(x)} \int_{-\infty}^x dx' e^{-\beta U(x')} \right]^{-1} \quad (5.4)$$

For a single degree of freedom with a high barrier the rate constant becomes

$$k_{\text{SD}} \sim k_{\text{TST}}(\omega_B / \gamma) \quad (5.5)$$

This is the high-friction limit of the Kramers result¹

$$k = k_{\text{TST}} [1 + (\gamma / 2\omega_B)^2]^{1/2} - \gamma / 2\omega_B \quad (5.6)$$

which reduces to transition-state theory at small friction. Alternatively, for a cusped barrier, which is common in reactions involving electronic curve crossing,^{121,122} (5.4) results in

$$k_{\text{SD}} \sim k_{\text{TST}}(\omega_0 / \gamma)(\pi\beta Q)^{1/2} \quad (5.7)$$

One should note that (5.4) applies equally well to the case of many degrees of freedom and to a rotating molecule with the proper potential of mean force (section 2). In the case of a diatomic recombination reaction the effective potential is $U_{\text{eff}}(r) = U(r) - 2k_B T \log(r)$. If $U(r)$ vanishes for $r > a$ and is strongly attractive for $r < a$, (5.4) gives (5.3), the bimolecular Smoluchowski recombination rate constant.¹¹

All of the above results are for Markovian systems. Of course, a realistic solvent will have a finite relaxation time and therefore the constant zero frequency friction γ is unphysical and should be replaced by a time-dependent friction kernel $\zeta(t)$. The central equation is then the generalized Langevin equation^{4,87}

(117) Onsager, L. *Phys. Rev.* **1938**, *54*, 554.

(118) Debye, P. *Trans. Electrochem. Soc.* **1942**, *82*, 265.

(119) Northrup, S. H.; Hynes, J. T. *J. Chem. Phys.* **1979**, *71*, 871.

(120) Skinner, J. L.; Wolynes, P. G. *Physica A (Amsterdam)* **1979**, *96A*, 561.

(121) Tully, J. C. In *Dynamics of Molecular Collisions, Part B*; Miller, W. H., Ed.; Plenum: New York, 1976.

(122) Garg, A.; Onuchic, J. N.; Ambegaokar, V. *J. Chem. Phys.* **1985**, *83*, 4491.

(112) Matkowsky, B. J.; Schuss, Z. *SIAM J. Appl. Math.* **1983**, *43*, 673.

(113) Sceats, M. G. *Chem. Phys. Lett.* **1986**, *128*, 55.

(114) Hippler, H.; Schranz, H. W.; Troe, J. *J. Phys. Chem.* **1986**, *90*, 6158.

(115) Schranz, H. W.; Troe, J. *J. Phys. Chem.* **1986**, *90*, 6168.

(116) Straub, J. E.; Borkovec, M.; Berne, B. J., submitted for publication in *J. Chem. Phys.*

$$\mu \ddot{x} = -\partial U(x)/\partial x - \int_0^t \zeta(t-t') \dot{x}(t') + R(t) \quad (5.8)$$

where x is the reaction coordinate feeling a potential $U(x)$, μ is the reduced mass, and $R(t)$ is a stochastic force which, along with the friction kernel $\zeta(t)$, must satisfy the fluctuation dissipation relation.

While attempts have been made to formulate a non-Markovian version of (5.4), nothing so general has been found.^{5,123} However, the problem was approximately solved by expanding the potential in the barrier region as an inverted parabola with frequency ω_B and assuming a steady-state distribution outside the barrier region. Grote and Hynes first obtained the rate constant^{57,124} which has since been derived in a number of different formulations^{53,123} and contexts.^{5,33,125,126} It is given by

$$k_{GH} = k_{TST}(\lambda/\omega_B) \quad (5.9)$$

where it can be shown¹²⁷ that, unless the bath contains unstable modes, λ is the only positive root of the Grote-Hynes relation

$$\lambda^2 + \lambda \tilde{\zeta}(\lambda) = \omega_B^2 \quad (5.10)$$

where $\tilde{\zeta}(s)$ is the Laplace transform of the friction kernel on the reaction coordinate per unit mass. k_{TST} is the transition-state result applied to the one-dimensional reaction coordinate (section 2). Recently, Bergsma et al. calculated rate constants numerically for an atom-transfer reaction in water and found non-Markovian effects to be quite important.⁶⁸ The Grote-Hynes theory has usually been used to give a reliable prediction of the numerical data.¹²⁸

If the friction kernel is frequency independent, i.e., $\tilde{\zeta}(0) = \gamma$, then the Grote-Hynes relation reduces to the Kramers result, (5.6). This result has been applied to a wealth of chemical systems; there exist reviews summarizing this work.^{3,4}

To successfully apply these theories to real systems, one must have knowledge of the dynamic friction coefficient, $\zeta(t)$, acting on the reaction coordinate. Unfortunately, even the static friction coefficient is not known, nor are there practical theoretical models for it for realistic systems.

The generalized Langevin equation, (5.8), cannot be derived in general from classical or quantum dynamics. It is usually assumed to apply without questioning its validity. For nonlinear systems it is not at all clear when this equation will be valid even in simple cases. It has been derived for an anharmonic oscillator coupled to a harmonic bath.¹²⁹ In this case, the dynamical friction has the simple form, for an infinite bath

$$\zeta(t) = \int d\omega \frac{J(\omega)}{\omega^2} \cos(\omega t) \quad (5.11)$$

and for a discrete bath

$$\zeta(t) = \sum_{\alpha} (g_{\alpha}^2/m_{\alpha}\omega_{\alpha}^2) \cos(\omega_{\alpha}t) \quad (5.12)$$

Here, g_{α} is the coupling constant of the reaction coordinate to the bath, m_{α} and ω_{α} are the masses and frequencies of the harmonic bath mode α , and $g_{\alpha}^2/m_{\alpha}\omega_{\alpha}^2$ is independent of the bath masses, m_{α} , because $m_{\alpha}\omega_{\alpha}^2$ is a mass-independent force constant. The only mass dependence arises from the frequency factors, ω_{α} , in the cosines, which are proportional to $m_{\alpha}^{-1/2}$. Thus if the solvent mass is changed relative to the solute mass, only the time scale will change; that is, there should be no change in the overall functional form of $\zeta(t)$. Clearly there is no dependence of $\zeta(t)$ on the reaction coordinate itself.

Recently, we have developed a method for computing $\zeta(t)$ on a reaction coordinate using molecular dynamics simulations.¹³⁰

(123) Hänggi, P.; Mojtabai, F. *Phys. Rev. A* **1982**, *26*, 1168.

(124) Grote, R. F.; Hynes, J. T. *J. Chem. Phys.* **1981**, *74*, 4465.

(125) Wolynes, P. G. *Phys. Rev. Lett.* **1981**, *47*, 968.

(126) Hänggi, P.; Grabert, H.; Ingold, G. L.; Weiss, U. *Phys. Rev. Lett.* **1985**, *55*, 761.

(127) Grabert, H., private communication.

(128) Gertner, B. J.; Bergsma, J. P.; Wilson, K. R.; Lee, S.; Hynes, J. T. *J. Chem. Phys.* **1987**, *86*, 1377.

(129) Zwanzig, R. *J. Stat. Phys.* **1973**, *9*, 215.

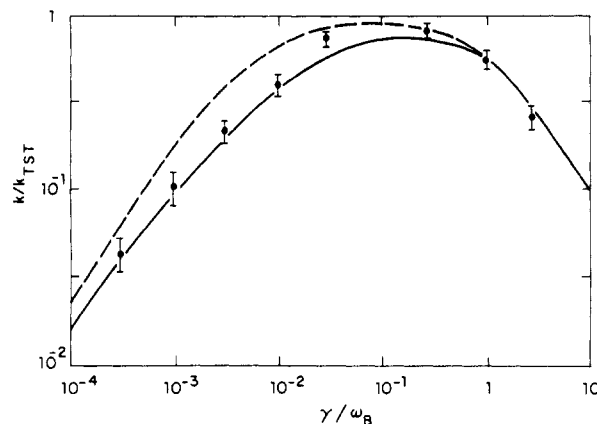


Figure 8. Log-log plot of the rate constant as a function of the static friction γ in units of the barrier frequency ω_B for the Kramers model for a two degree of freedom potential. Displayed are the predictions of (6.1) (---) and (6.2) (—) alongside numerical simulation results.¹⁰³

This method allows one to test the range of validity of the above equations. We have applied it to a simple bistable system dissolved in Lennard-Jonesium. It was found that $\zeta(t)$ depends on the reaction coordinate in contradiction to the above generalized Langevin equation. Moreover, the time dependence does not scale simply as the square root of the solvent mass.

Clearly, one must be cognizant of the limitations of these theories when comparing them to experiment. It may well be necessary to derive a generalized Langevin equation that is nonlocal in space as well as time for applications to some problems.

6. Connection Formulas

Until now we have discussed theories which correct for deviations from transition-state theory in the form of rate constants for energy activation at low collision rates (section 4) and spatial diffusion at high collision rates (section 5). Any of these theories are only correct in certain limits. Obviously, one is interested in predicting the rate constant at arbitrary collision rate, or friction constant. One useful approximation, first proposed by Hynes and co-workers,^{4,99} is

$$k^{-1} \simeq k_{\text{low}}^{-1} + k_{GH}^{-1} \quad (6.1)$$

where k_{low} is the rate for energy activation (eq 4.7) and k_{GH} is the Grote-Hynes theory rate for barrier crossing, (eq 5.9). We may also use^{17,131}

$$k \simeq k_{\text{uni}}k_{GH}/k_{TST} \quad (6.2)$$

The latter is highly preferable in systems with many intramolecular degrees of freedom when a good approximation to the unimolecular rate theory expression k_{uni} , (4.5), is at hand. Differences between the stable-states formula (6.1) and the product approximation (6.2) can be substantial in the low to intermediate friction regimes for many degrees of freedom and the latter should always be preferred.¹⁰³

For atom-transfer reactions the activation step is missing and a useful approximation is

$$k \simeq k_{GH} \quad (6.3)$$

Some justification for these formulas can be given by analyzing the steady state of the Lindemann mechanism (see section 1), asymptotic techniques,^{132,133} or stable-states arguments.³¹ These formulas can give accurate predictions; nevertheless, they are approximate. For example, in Figure 7 we compare the prediction of (6.1) for the BGK model for a bistable mode coupled to a nonreactive mode. On the other hand, (6.1) fails badly for the Kramers model on the same surface whereas (6.2) is a good

(130) Straub, J. E.; Borkovec, M.; Berne, B. J. *J. Phys. Chem.* **1987**, *91*, 4995.

(131) Troe, J. *J. Phys. Chem.* **1986**, *90*, 357.

(132) Matkowsky, B. J.; Schuss, Z.; Tier, C. *J. Stat. Phys.* **1984**, *35*, 443.

(133) Dygas, M. M.; Matkowsky, B. J. *J. Chem. Phys.* **1986**, *84*, 3731.

approximation¹⁰³ (see Figure 8).

6.1. Simulations. For Markovian models and strongly coupled degrees of freedom we expect that an interpolation formula which approximately includes the unimolecular RRKM-theory result, (4.5), and the diffusion-controlled theory should be able to predict the overall rate constant quite accurately. Certainly, such formulas are much simpler to use than alternative methods such as Padé approximants^{90,94} or matching solutions¹³⁴ and they give essentially identical results. On the other hand, when strongly non-Markovian baths or weakly coupled degrees of freedom are included, such formulas are expected to be much less reliable. It is known that in some cases no existing analytic theories will describe such situations. Let us briefly discuss two examples.

We have studied a single reactive degree of freedom experiencing exponential friction.^{73,74} We found that in the high-friction, long correlation time regime the interpolation formula (6.1) can severely overestimate the rate constant. Deviations from (6.1) arise from the breakdown of the assumption that trajectories, after leaving the barrier region, will be deactivated before recrossing the transition state. Physically, the recrossings are due to the long relaxation time of the solvent which cages the activated particle in an effective double well potential.⁷⁴ We can think of this cage arising from a frozen solvent configuration. The rigid solvent causes the particle to rebound and recross the transition state. Therefore, the particle's dynamics is affected by anharmonic regions of the potential not included in the Grote-Hynes or energy activation theories. We feel that while the particle is caged, the slow variable is the energy, not the position, and therefore energy activation in the dynamic potential must be included.

One attempt to correct (6.1) has treated only the position as a slow variable¹³⁵ and therefore has not, as has been suggested,¹³⁶ accounted for these deviations. Zwanzig has recently used ideas from singular perturbation theory to arrive at limits on the range of friction where Grote-Hynes theory can be expected to work.¹³⁷ Similar limits have been suggested by Hänggi.⁵ In this range of friction, the probability that the trajectory samples the anharmonic regions of the potential is negligible. Also, he showed that in the limit where Grote-Hynes theory is not appropriate there is, in addition to the energy, a second conserved quantity corresponding to the relaxation of the dynamic potential, which must be treated if the rate constant is to be calculated accurately. A recent study has included the continued relaxation of these two conserved quantities in the calculation of rate constants.¹³⁸

In another study of a non-Markovian system, an oscillatory friction kernel was used which corresponded exactly to a linearly coupled damped harmonic oscillator.⁷⁵ Rate constants were correctly predicted by energy diffusion theories using (4.17) and (4.22) for $n = 1$ as long as the friction kernel decayed rapidly, i.e., at large damping. On the other hand, if the friction kernel becomes oscillatory, i.e., at low damping, this prediction and therefore also the stable-states formula, (6.1), severely underestimates the rate constant. In this case, the bath, i.e., the linearly coupled harmonic oscillator, becomes strongly coupled to the reaction coordinate and the rate constant is better described by (4.21) for $n = 2$. Therefore, for a given collision kernel, it is not trivial to decide whether the coupling can be regarded as weak enough that (4.22) can be applied. We have presented sufficient conditions for resolving this question^{75,103} which have been further sharpened by Nitzan.¹³⁶

These two examples illustrate that many features of non-Markovian activation rate processes are still not well understood and deserve much effort in future research.

6.2. Electronic Surface Crossing. In our previous discussion, we have assumed that the electronic state of the reacting molecule

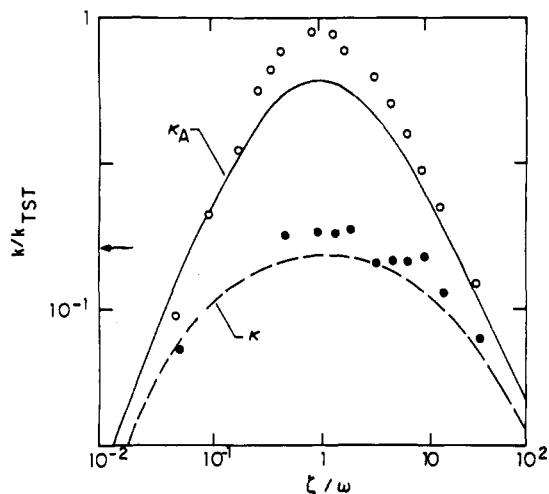


Figure 9. Log-log plot of the transition-state-theory normalized rate constant as a function of the collision frequency ζ in units of the well frequency ω for the adiabatic theory (—) and the nonadiabatic theory (---) of (6.4). The simulation results of Cline and Wolynes¹⁴¹ are shown for the adiabatic (O) and nonadiabatic (●) systems. The maximum nonadiabatic transmission coefficient, predicted by (6.4), is indicated by an arrow.

follows the motion of the nuclei adiabatically. However, when the splitting between the excited- and ground-state adiabatic potential energy surfaces is small compared to $k_B T$, the assumption of adiabatic curve crossing may be violated. For isolated systems, nonadiabatic curve crossing effects have been incorporated statistically by using Landau-Zener theory in semiclassical trajectory calculations by Tully and Preston¹³⁹ and Miller and George,¹⁴⁰ this and additional work have been reviewed by Tully.¹²¹ Recently, Cline and Wolynes employed similar numerical techniques to study nonadiabatic effects on activated barrier crossing.¹⁴¹

Extending the absorbing boundary formalism (section 3), we have combined surface crossing, using the Landau-Zener curve-crossing probability,¹²¹ with our model of adiabatic reaction dynamics.⁷⁰ The resulting transmission coefficient for the non-adiabatic rate process is¹⁴²

$$\kappa^{-1} = \frac{1 - \overline{P_{LZ}}}{2\overline{P_{LZ}}} + \kappa_A^{-1} \quad (6.4)$$

where κ_A is the transmission coefficient for the adiabatic reaction, (3.9), and $\overline{P_{LZ}}$ is the Landau-Zener curve crossing probability¹²¹ averaged over the distribution of (3.6).

In the adiabatic limit, $\overline{P_{LZ}} = 1$ and $\kappa = \kappa_A$. If $\kappa_A \ll \overline{P_{LZ}}$, then $\kappa \sim \kappa_A$ which is the asymptotic adiabatic result.^{122,143} Equation 6.4 predicts a maximum transmission coefficient of $\kappa = 2\overline{P_{LZ}}/(1 + \overline{P_{LZ}})$ which, for $\overline{P_{LZ}} \ll 1$, reduces to $\kappa = 2\overline{P_{LZ}}(1 - \overline{P_{LZ}})$.¹²¹ Physically, a small Landau-Zener curve-crossing probability can be understood as a density-independent rate-limiting step below TST. This behavior is illustrated in Figure 9.

It should be noted that (6.4) only requires a knowledge of the Landau-Zener probability and the adiabatic rate constant, which may be determined by computer simulation or analytic theory. We have compared (6.4) with the numerical simulation results of Cline and Wolynes, which included curve crossing with BGK collisional dynamics. Using the analytic theory of Skinner and Wolynes⁹⁴ for κ_A , we found good agreement.¹⁴²

7. Experimental Results

There have been a vast number of experimental studies of how rate constants depend on the medium.^{4,17} With the limited space

(134) Carmeli, B.; Nitzan, A. *J. Chem. Phys.* **1984**, *80*, 3596.

(135) Okuyama, S.; Oxtoby, D. *J. Chem. Phys.* **1986**, *84*, 5824. *Ibid.* **1986**, *84*, 5830.

(136) Nitzan, A. *Non-Markovian Theory of Activated Processes. VI. Unimolecular Reactions in Condensed Phases.* (preprint).

(137) Zwanzig, R. *J. Chem. Phys.* **1987**, *86*, 5801.

(138) Talkner, P.; Braun, H. B. *Transition Rates of a Non-Markovian Brownian Particle in a Double Well Potential.*

(139) Tully, J. C.; Preston, R. K. *J. Chem. Phys.* **1971**, *55*, 562.

(140) Miller, W. H.; George, T. F. *J. Chem. Phys.* **1972**, *56*, 5637.

(141) Cline, R. E., Jr.; Wolynes, P. G. *J. Chem. Phys.* **1987**, *86*, 3836.

(142) Straub, J. E.; Berne, B. J. *J. Chem. Phys.* **1987**, *87*, 6111.

(143) Frauenfelder, H.; Wolynes, P. G. *Science (Washington, D.C.)* **1985**, *229*, 337.

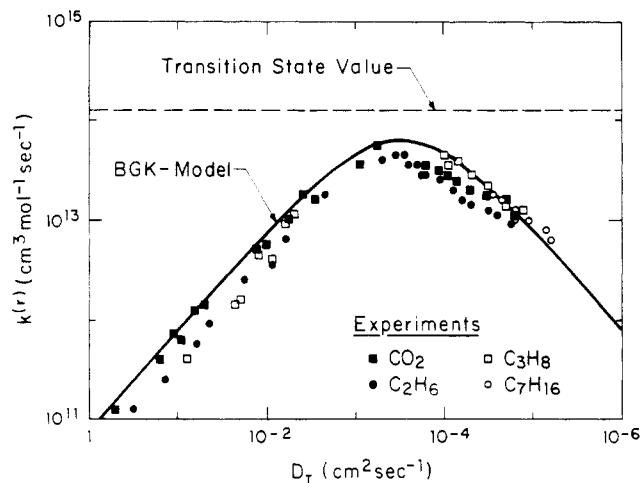


Figure 10. Troe and co-workers' experimental data¹⁵⁰ for the recombination of iodine as a function of the diffusion coefficient for a single iodine atom compared with the impulsive BGK model without adjustable parameters (—).¹¹

available it is not possible to review this field appropriately. Instead, we would like to make some specific comments and focus on three examples which we consider particularly relevant. The most severe problem when one tries to compare theory and experiment is that, because of experimental difficulties, data are usually collected over a very limited range of pressure or viscosity. In such cases, there is usually a small variation in the rate constant and virtually any theory showing the same qualitative behavior can be used to fit the data. Avoiding this difficulty, we restrict our discussion to a few relevant experiments where rate constants have been measured over a wide density range.

Another important aspect which must be carefully addressed when comparing experiments and theories is the effects of the potential of mean force. The experimentally observed rate constants contain not only dynamic effects, in the form of diffusion control and energy activation, but also equilibrium solvent effects (solvent shifts) manifest in variations of the barrier height, due to the potential of mean force. Very often these effects are not properly disentangled and can lead to erroneous conclusions. A particularly nice example was discussed by Hicks et al.¹⁶ where a rate constant showed a phenomenological inverse dependence on the solvent viscosity. The immediate conclusion—diffusion-controlled reaction—is wrong! Careful study of the temperature dependence of the rate constant in isoviscous solvents of different polarity shows clearly¹⁶ that this variation of the rate constant is caused by a polar equilibrium effect.

Additionally, it is crucial to estimate correctly the friction on the reaction coordinate. It should be noted that the often-used Stokes-Einstein relation, where the friction is $\zeta = 6\pi\eta a$, has a limited range of validity.¹⁴⁴⁻¹⁴⁸

7.1. Halogen Recombination. The first and simplest experimental rate studies involved halogen recombination reactions. The recombination rate constant can be measured over a wide range of densities and in different bath gases.¹⁴⁹⁻¹⁵¹ Such studies on chlorine¹⁴⁹ were the first to show a certain turnover of the rate constant as a function of density.¹⁵² Ironically, these results remained unnoted for a decade until the studies were extended to other halogens.^{150,151} The typical picture for iodine (Figure

10) clearly displays the turnover as a function of density.¹⁵⁰ The theoretical prediction using the BGK model gives very good agreement.¹¹ This agreement is somewhat fortuitous in the low-pressure regime since this model as well as the Kramers model¹⁵³ does not predict the correct temperature dependence of the rate constant which is dominated again by a complex reaction mechanism not included in the model.¹¹

At high pressures the rate constant seems to fall off more slowly than the inverse viscosity which is probably due to the failure of the Stokes-Einstein relation.¹⁴⁴⁻¹⁴⁷ A similar situation is encountered in polyatomic radical recombination where the rate constant is well described by a diffusion-controlled model but the predictions of the Stokes-Einstein relation are not very accurate.¹⁵⁴ Equilibrium solvent effects are small in this particular case.¹¹ Studies of such secondary recombination should not be confused with primary recombination reactions where the iodine relaxes from an electronically excited state.¹⁵⁵ In the latter case there is no separation of time scales and the ideas presented here do not apply except in a strongly modified form.

7.2. Stilbene Isomerization. Another well-studied system is stilbene isomerization on an excited electronic surface.¹⁵⁶⁻¹⁵⁹ This reaction shows a clear turnover as a function of density. Equilibrium solvent effects due to the potential of mean force are very important in this case. This is to be expected since the electronically excited stilbene is probably highly polar and is therefore interacting strongly with the solvent. Studies of the temperature dependence of the rate constant,^{160,161} and the fact that the maximum rate constant exceeds the transition-state rate constant calculation for the isolated molecule, using (4.11), by 2 orders of magnitude,¹⁵⁶ show clearly that the barrier is substantially modified as the density of the solvent is changed. Therefore, any extensive comparison with dynamic theories which does not assess the equilibrium solvent effects is obsolete^{114,115,162}—a fact repeatedly emphasized by Troe.

Similarly, Pollak has considered the very different high-density viscosity dependence of two harmonic Hamiltonians. Using a hybrid of these Hamiltonians, he found that an increase in the viscosity corresponds to a lower barrier to isomerization which fits well the high density falloff in stilbene.¹⁶³ Pollak's interpolation is similar to an equilibrium solvent effect since his effective potential varies with the damping. Unfortunately, since the interaction of an excited solute with the solvent is hard to establish, it is very difficult to make any quantitative prediction of the equilibrium solvent effect. For example, a recent study has shown that a high-density fractional viscosity dependence can result from strongly anisotropic diffusion.¹⁶⁴ In our view, there is no conclusive evidence for the importance of non-Markovian effects in the stilbene isomerization.

7.3. Cyclohexane Isomerization. A system where estimation of equilibrium solvent effects is more tractable is the cyclohexane isomerization. This system was initially studied by Jonas and co-workers at high pressure where, for the first time, Kramers' ideas were applied to a realistic chemical reaction.¹⁰⁸ Subsequent work extended the pressure range studied to lower pressures.¹⁰⁷ Garrity and Skinner¹⁶⁵ discuss the possible importance of a

(144) Pollack, G. L. *Phys. Rev. A* **1981**, *23*, 2660.
 (145) Pollack, G. L.; Eneyart, J. *J. Phys. Rev. A* **1985**, *31*, 980.
 (146) Tyrrell, H. J. V.; HARRISS, K. R. *Diffusion in Liquids*; Butterworths: London, 1984; Vol. 66, Chapter 7.2.
 (147) Zwanzig, R.; Harrison, A. K. *J. Chem. Phys.* **1986**, *83*, 5861.
 (148) Hippler, H.; Troe, J. *Ber. Bunsen-Ges. Phys. Chem.* **1985**, *89*, 760.
 (149) Hippler, H.; Troe, J. *Int. J. Chem. Kinet.* **1976**, *8*, 501.
 (150) Otto, B.; Schroeder, J.; Troe, J. *J. Chem. Phys.* **1984**, *81*, 202.
 (151) Hippler, H.; Schubert, V.; Troe, J. *J. Chem. Phys.* **1984**, *81*, 3931.
 (152) The turnover in chlorine appears at unusually low pressures and is probably due to a second competing reaction channel.¹⁵⁶

(153) Sceats, M. G.; Dawes, J. M.; Millar, D. P. *Chem. Phys. Lett.* **1985**, *114*, 63.

(154) Schuh, H.; Fischer, H. *Helv. Chim. Acta* **1978**, *61*, 2130.

(155) Chuang, T. J.; Hoffman, G. W.; EISENTHAL, K. B. *Chem. Phys. Lett.* **1974**, *25*, 201.

(156) Mancke, G.; Schroeder, J.; Troe, J.; Voss, F. *Ber. Bunsen-Ges. Phys. Chem.* **1985**, *89*, 896.

(157) Fleming, G. R.; Courtney, S. H.; Balk, M. W. *J. Stat. Phys.* **1986**, *42*, 83.

(158) Lee, M.; Holtom, G. R.; Hochstrasser, R. M. *Chem. Phys. Lett.* **1985**, *118*, 359.

(159) Lee, M.; Bain, A. J.; McCarthy, P. J.; Han, C. H.; Haseltine, J. N.; Smith, A. B., III; Hochstrasser, R. M. *J. Chem. Phys.* **1986**, *85*, 4341.

(160) Sundström, V.; Gillbro, T. *Chem. Phys. Lett.* **1984**, *109*, 538.

(161) Sundström, V.; Gillbro, T. *Ber. Bunsen-Ges. Phys. Chem.* **1985**, *89*, 222.

(162) Schroeder, J.; Troe, J. *Chem. Phys. Lett.* **1985**, *116*, 453.

(163) Pollak, E. *J. Chem. Phys.* **1987**, *86*, 3944.

(164) Agmon, N.; Kosloff, R. *J. Phys. Chem.* **1987**, *91*, 1988.

two-dimensional surface for this system, and Carmeli and Nitzan¹⁶⁶ have interpreted this in terms of a non-Markovian generalized Langevin equation.

Recently, Singer, Kuharski, and Chandler¹⁶⁷ estimated the equilibrium solvent effect to be $\Delta V_{\text{TST}} \approx 0.6 \text{ cm}^3/\text{mol}$. This estimate is just the opposite of Jonas's estimate $\Delta V_{\text{TST}} \approx -1.5 \text{ cm}^3/\text{mol}$ which is based on the approximation of hard sphere interactions. It seems that the interactions present in this nonpolar system, which are comparable with thermal energies, cannot be approximated by using the intuitive concept of reactant volume changes. Therefore, the data on cyclohexane imply that the transmission coefficient κ increases with pressure over the whole density range in contrast to the widely accepted interpretation by Jonas which predicts a decreasing κ going through a maximum.

A slowly increasing κ could be caused by two effects and possibly a combination thereof. First, it is known that RRKM weak collision models show a very smooth transition between their low-pressure limit and transition-state theory^{11,91,102} (section 4). Second, the presence of weakly coupled modes in the molecule could cause a transition to a quasi few degree of freedom system at higher

pressures.^{19,75,76,103} As mentioned in section 4.4, recent work confirms this prediction.^{109,110} As the calculation of the potential of mean force is hard but feasible, it would be extremely helpful to collect more extensive data on this system covering a wide density and temperature range. In conclusion, the data on cyclohexane still await a definitive interpretation.

Our three examples show that, while these are the systems best understood, having been in the focus of study for many years, there exist many uncertainties. In our view, the weak points on the experimental side are that systems are not studied over a wide enough range of densities, temperatures, and solvents. It is also desirable to extend such studies to atom-transfer and polyatomic recombination reactions. On the theoretical side, a small knowledge of the true intramolecular solute potential and the solvent-solute potential makes application of existing theories difficult. Practical procedures for calculating rate constants in polyatomics at low pressures beyond the strong collision approximation, which would take the proper collisional dynamics into account, are still lacking. Finally, ways of incorporating different reaction channels, quantum effects, and all electronic surfaces participating are in their infancy.

Acknowledgment. We thank J. Troe, D. Chandler, P. Hänggi, P. Talkner, D. Thirumalai, H. Grabert, J. Skinner, D. Hsu, and M. Sceats for helpful discussion and correspondence.

(165) Garrity, D. K.; Skinner, J. L. *Chem. Phys. Lett.* **1983**, *95*, 46.

(166) Carmeli, B.; Nitzan, A. *Chem. Phys. Lett.* **1984**, *106*, 329.

(167) Singer, S. J.; Kuharski, R. A.; Chandler, D. *J. Chem. Phys.* **1986**, *90*, 6015.

ARTICLES

Rotational Effects on Intramolecular Radiationless Transitions. The Story of Pyrazine

Aviv Amirav

School of Chemistry, Sackler Faculty of Exact Sciences, Tel Aviv University, Ramat Aviv 69978 Tel Aviv, Israel (Received: June 8, 1987; In Final Form: November 13, 1987)

The experimental rotational effects on the $S_1(^1B_{3u})$ excited-state dynamics of pyrazine are briefly summarized. These experiments impose severe constraints on the validity of the general radiationless transitions theory in the limit of intermediate level structure. A model is presented to account for all the problems confronted by the theory in terms of rotationally induced intratriplet vibrational energy redistribution. This new type of intramolecular radiationless transition called vibrational crossing is an interstate process with intrastate vibronic coupling features. From this model two major predictions emerge, which are shown to be fulfilled. We demonstrate that Coriolis coupling is an important and dominant mechanism leading into intramolecular vibrational energy redistribution. The absorption spectrum, fluorescence excitation spectrum, and the resulting emission quantum yield of pyrazine were studied by using dye laser with 2-GHz resolution as a light source. The emission quantum yield decreased with the rotational state. The absorption contour of a single rotational state was broader than the excitation contour, and absorption with a low emission quantum yield is shown between adjacent rotational transitions. The ratio of short time to long time emission (A^+/A^-) is shown to depend on the rotational temperature following excitation of a single rotational transition. These experimental results combined with the quantitative fit of the inverse emission quantum yield and A^+/A^- were predicted by the vibrational crossing model and thus strongly support its validity.

Introduction

The $S_1(^1B_{3u})$ state of the pyrazine molecule serves as a touchstone for critical scrutiny of the theory of radiationless transitions.¹⁻⁵ Following the pioneering work of Tramer and co-workers,^{6,7} conventional wisdom has attributed intramolecular

dynamics in this system to the intermediate level structure (ILS) limit in the theory.¹⁻⁷ As detailed experimental results have become available, this picture became less clear and understandable as the conventional theory in the ILS limit was confronted with a large volume of conflicting pieces of experimental results. These puzzling self-inconsistencies are described in detail elsewhere.⁸

(1) Bixon, M.; Jortner, J. *J. Chem. Phys.* **1968**, *48*, 715.
 (2) Bixon, M.; Jortner, J.; Dothan, Y. *Mol. Phys.* **1969**, *17*, 109.
 (3) Jortner, J.; Mukamel, S. In *Molecular Energy Transfer*; Levine, R. D., Jortner, J., Eds.; Wiley: New York, 1979; p 178.
 (4) Jortner, J.; Levine, R. D. *Adv. Chem. Phys.* **1982**, *47*, 1.
 (5) Nitzan, A.; Jortner, J.; Rentzepis, P. M. *Proc. R. Soc. London*, **A 1972**, *327*, 367.

(6) Frad, A.; Lahmani, F.; Tramer, A.; Tric, C. *J. Chem. Phys.* **1974**, *60*, 4419.
 (7) Lahmani, F.; Tramer, A.; Tric, C. *J. Chem. Phys.* **1974**, *60*, 4431.
 (8) Amirav, A. *Chem. Phys.* **1986**, *108*, 403.